Psychophysical Channels and the Physiology of Perception in the Rat Whisker System

Dissertation

zur Erlangung des Grades eines Doktors
der Naturwissenschaften

der Fakultät für Biologie
und
der Medizinischen Fakultät
der Eberhard-Karls-Universität Tübingen

vorgelegt
von

Maik Christopher Stüttgen
aus Köln, Deutschland

März 2007

Tag der mündlichen Prüfung:	12.10.2007
Dekan der Fakultät für Biologie:	Prof. Dr. F. Schöffl
Dekan der Medizinischen Fakultät:	Prof. Dr. I. B. Autenrieth
1. Berichterstatter:	PD Dr. Cornelius Schwarz
2. Berichterstatter:	Prof. Dr. Hans-Ulrich Schnitzler
3. Berichterstatter:	Prof. Dr. Carl Petersen
Prüfungskommission:	PD Dr. Cornelius Schwarz
	Prof. Dr. Hans-Ulrich Schnitzler
	Prof. Dr. Carl Petersen
	Prof. Dr. Christoph Braun
	Prof. Dr. Peter Thier

Meinen Eltern

Contents

Abstract

The rat whisker system has evolved into in an excellent model system for sensory processing from the periphery to cortical stages. However, to elucidate how sensory processing finally relates to percepts, methods to assess psychophysical performance pertaining to precise stimulus kinematics are needed. This dissertation describes a head-fixed, behaving rat preparation that allows to measure detectability of a single whisker deflection as a function of amplitude and velocity.

A behavioral study employing the psychophysical detection task showed that velocity thresholds for detection of small-amplitude stimuli ($< 3°$) were considerably higher than for detection of large-amplitude stimuli ($> 3°$). This finding suggests the existence of two psychophysical channels mediating detection of whisker deflection: one channel exhibiting high amplitude and low velocity thresholds (W1), and the other channel exhibiting high velocity and low amplitude thresholds (W2). The correspondence of W1 to slowly adapting (SA) and W2 to rapidly adapting (RA) classes of primary afferents in the trigeminal ganglion was revealed in acute neurophysiological experiments. Neurometric plots of SA and RA cells were closely aligned to psychophysical performance in the corresponding W1 and W2 parameter ranges. Interestingly, neurometric data of SA cells fit the behavior best if it was based on a short window integrating action potentials during the initial phasic response, in contrast to integrating across the tonic portion of the response.

To further elucidate sensory processing in the W1 channel, I performed neurophysiological recordings across all layers of barrel cortex in rats trained on the psychophysical detection paradigm. The whisker deflection kinematics were tailored to isolate the W1 channel. Neurometric curves derived from either single or multi unit activity in barrel cortex were less or equally sensitive to whisker deflections than the organism itself. This supports a "lower envelope" model of detection, in which perception of a faint stimulus is mediated by the most sensitive neurons available rather than average neuronal activity. In a next step, I checked whether any trial-by-trial covariation existed between neuronal activity and the report of a percept ("choice probability"). While the recordings displayed a wide range of choice probabilities, they clustered around the value expected by chance. Moreover, individual neurons' sensitivity and their associated choice probability did not show a substantial correlation. This is at odds with a lower envelope account, because this predicts that the most sensitive neurons should have the largest choice probabilities. Nonetheless, these observations suggest that the lower envelope model, while untenable in its stringent form, still provides a more satisfying description of the neural processes underlying detection of faint stimuli in the rat whisker system than alternative response pooling accounts.

1 Overall introduction

1.1 The rat whisker system

The whisker-to-barrel pathway is widely studied as a model system of tactile information processing (Sachdev et al., 2001) and is reportedly the most frequently investigated mammalian sensory system after the visual system of primates (Jones & Diamond, 1995).

In rats, the large mystacial whiskers ("macrovibrissae"; Brecht et al., 1997) are arranged in a highly stereotypic pattern on both sides of the muzzle. Accordingly, they can easily be identified as belonging to one of five rows labeled A to E and one of the (approximately) five arcs, labeled 1 to 5 (Figs. 1ab). Whiskers exhibit an exponential length decrease from caudal to rostral, ranging from several centimeters down to a few millimeters only. At the rostral pole of the snout, the macrovibrissae are becoming more and more the "microvibrissae", very fine, short hairs, about which little is known. Additionally, rats have an additional caudal arc of four whiskers, slightly displaced ventrally with respect to the rows. These four whiskers are called "straddlers", and labeled α, β, γ, and δ, according to their proximities to rows A, B, C, and D, respectively. Importantly, whiskers are not passive appendages. During exploration, rats rhythmically sweep their whiskers at a frequency between five and eleven Hertz, a behavior called "whisking" (Welker, 1964).

The most prominent feature of the whisker system is the somatotopic map discovered in the primary somatosensory cortex. Similar to the highly ordered arrangement on the snout, there exist cortical columns, each of which corresponds to one of the mystacial whiskers (Woolsey & van der Loos, 1970); Welker, 1971). The arrangement of whiskers on the snout is well preserved on the cortical surface. Anatomically, staining for cytochrome oxidase and slicing the brain tangentially to the cortical surface reveals barrel-like structures resulting from heavy staining of the neurons in layer IV. Accordingly, this part of rat primary somatosensory cortex is termed "barrel cortex" (Fig. 1c). Physiologically, neurons in each barrel respond best to deflections of their corresponding whisker, having the shortest response latency and the largest response magnitude (Simons, 1985). Compared to the rest of the body surface, the overall area of cortex devoted to the processing of whisker-related signals is huge (Woolsey & van der Loos, 1970; Welker, 1971), which parallels the overrepresentation of the fingers and the face found in primate somatosensory cortex (Penfield & Rasmussen, 1950).

Not surprisingly, the somatotopic organization of whiskers is present at intermediate neuronal relay stations already. Structures corresponding to cortical barrels have been termed "barreloids" in the ventral posterior medial (VPM) thalamus (Simons & Carvell, 1989), and "barreletes" in the trigeminal brainstem complex (Jacquin et al., 1993).

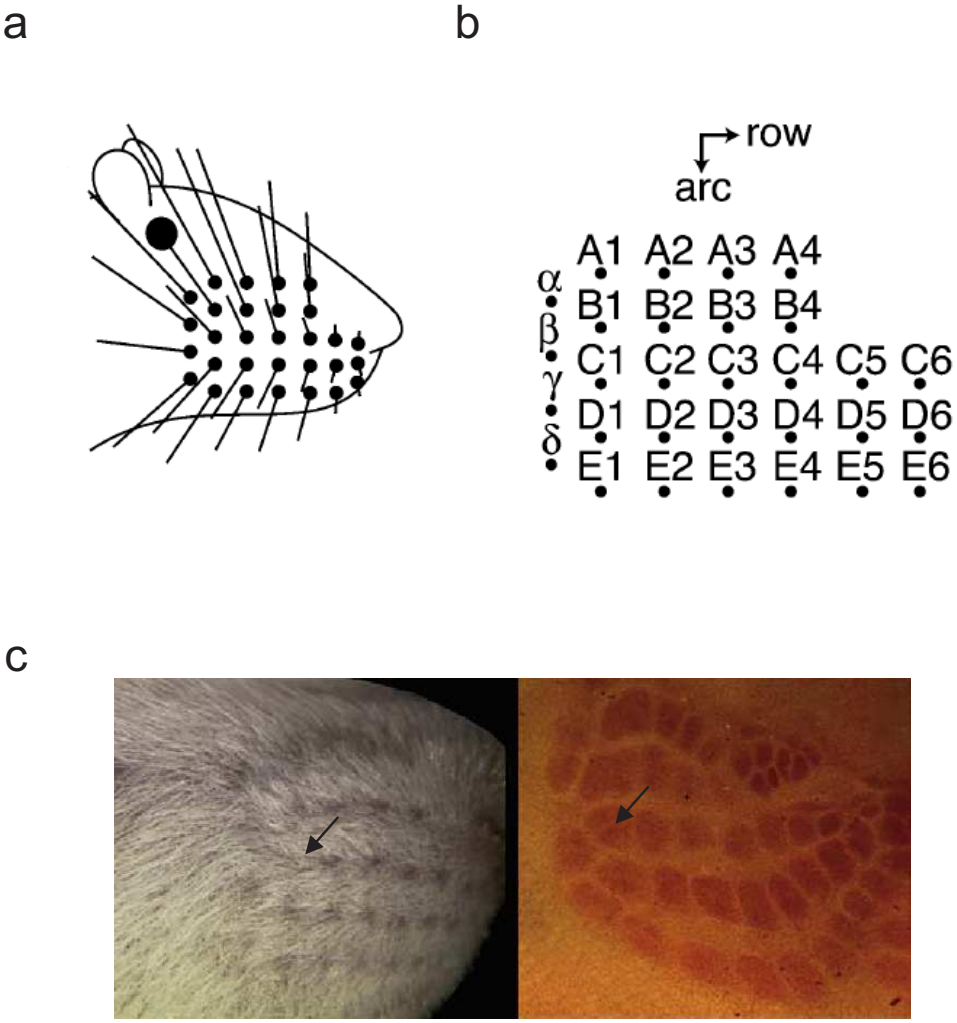

Figure 1: Whisker arrangement and cortical somatotopy. a) Sketch of whisker array on the snout of a rat. b) Idealized arrangement and labeling of whiskers. c) Left: picture of a rat snout with whisker follicles visible (dark, regularly ordered spots). Right: tangential cut through layer IV of the barrel cortex after staining for cytochrome oxidase. Arrows point to the C1 whisker follicle (left) and the C1 barrel (right). Adapted from Petersen (2003). Reprinted with kind permission of Springer Science and Business Media.

1.2 Behavioral studies of the rat whisker system

Compared to the abundance of anatomical and physiological data, behavioral evidence pertaining to the functional role of vibrissae in rats has been furnished by relatively few investigators. Early observations by Vincent (1912) in the laboratory of renowned behaviorist-psychologist John B. Watson inferred the importance of whiskers for the rat largely from behavioral impairments resulting from whisker clipping. She suggested that they represent "delicate tactile organs, which function in equilibrium, locomotion, and the discrimination of surfaces" (Vincent, 1912, p. 69). Vincent subjected rats to a maze-navigation task and observed progressive performance deficits with stepwise elimination of sensory cues. The rats were mildly food-deprived, and their task was to find the shortest way through the maze until they reached a food-cup. Vincent cut short the whiskers on either side of the face or both and observed dramatic increases both in runtimes as well as in errors (entering blind alleys) compared to untreated rats. These impairments were further aggravated by bilaterally cutting the infraorbital nerves, which transmit tactile sensation from the snout. (The experiments culminated when the animals were blinded by enucleation of their eyes and their whiskers were cut bilaterally. These animals never learned the task.)

Schiffman and colleagues (1970) probed the role of whiskers for depth perception. In a depth-discrimination task, rats were situated on a platform and given the opportunity to descend from the platform on either of two equally shallow sides. However, one of the two sides had a transparent floor; thus, if rats relied predominantly on vision to judge which of the two sides were shallower, they should exhibit a bias towards descending on the side with the opaque floor. The authors found that, while rats with intact vibrissae did not show such a bias, rats with their whiskers clipped did so, indicating that unaffected rats rely more on tactile than on visual clues to base their judgment.

In these and other studies, the central role of whiskers for the rat has been illustrated by cutting them off on one or both sides of the muzzle. As described above, whisker clipping on both sides of the face renders rats deficient in terms of orientation and equilibrium (Vincent, 1912); also, overall locomotion is markedly reduced (Richter, 1957; Griffiths, 1960). In addition, bilateral whisker clipping affects swimming capabilities: such animals swim less proficiently and tend to drown (Richter, 1957; Griffiths, 1960). Other investigators have reported increased "emotionality" (Gustafson & Felbain-Keramidas, 1977) in rats with bilaterally trimmed whiskers and suggested it was a result of frustration due to the inability of gathering information about the environment. Reported hints at increased arousal include increased defecation as well as greater resistance to handling (Hall, 1934). Even when only one side of the snout is subjected to whisker removal, rats show peculiar abnormalities. When scanning a novel environment, they tend to walk along the walls of that environment mostly with the whisker-intact side (Milani et al., 1989); this behavior persists for up to three days after hemivibrissotomy.

To complement paradigms relying on the effects of clipping whiskers to infer their function, some better controlled paradigms have been put forward more recently. These few psychophysical studies mostly used non-restrained, freely moving rats sampling stimuli by using own body and whisker movements. For example, in the "gap-crossing" paradigm used by Carvell & Simons (1990, 1995) and Guic-Robles et al. (1989, 1992), blindfolded rats are placed on an elevated start platform and have to decide on which of two target platforms to jump to obtain a food reward. The three platforms are spaced apart such that the rat can only touch the edges of either target platform when leaning forward over the gap and protracting the whiskers. The proximal edges of the target platforms exhibit differently coarse sandpaper surfaces. Either the rougher or the smoother surface is consistently found on the target platform with the food reward. After deciding which of the two platforms contains the rougher surface, rats jump over the gap to obtain the food. Carvell & Simons (1990) concluded from their data that rats are capable of fine-texture discriminations, with spatiotemporal resolution of the whisker tactile organs matching that of the primate fingertip.

While the gap-crossing paradigm ensures that the rat has to rely on its whiskers to decide which platform to jump on, it offers very little control over whisker stimuli. The animal itself is restricted in its explorative capabilities, because it has to constantly protract the whiskers in order to be able to palpate the surfaces. Also, the kinematic parameters impinging on the whiskers during palpation cannot be precisely manipulated. Videographic analysis of whisker motion is difficult to accomplish at a temporal and spatial resolution that allows to accurately track single whiskers in their three-dimensional movement patterns while they sweep across the surface.

Krupa et al. (2001) designed an aperture-discrimination task. Here, the rat enters a small "discrimination chamber" with its head to make a nose poke. At both sides of the nose poke, a variable width aperture is presented using movable side walls. Depending on whether the spacing between the two walls is narrow or wide, the rat is rewarded for making a consecutive nose poke at either of two reward stations located in a different chamber. While these investigators succeeded in measuring psychophysical discrimination thresholds (their best rats discriminated between 62 mm and 65 mm wide apertures), this paradigm suffers from similar limitations as the gap-crossing method. Again, it is the rat and not the experimenter who determines the exact whisker stimulus configuration and duration. Similar limitations apply to two other novel psychophysical paradigms (Knutsen et al., 2006; Mehta et al., 2007) in which rats discriminate horizontal object locations.

Hutson and Masterton (1986) are the only investigators so far who attempted to quantify psychophysical detection thresholds with varying kinematic deflection parameters. In their paradigm, rats are not whisking, and all but one whisker is clipped. Whisker deflections result from sinusoidally modulated air currents directed onto the whisker tip. The air current is applied constantly while the animal licks off

a spout to obtain a water reward on a variable-interval schedule. A change in the amplitude or frequency of the air current acts as a conditioned stimulus signaling an impeding foot shock, which temporarily suppresses licking ("conditioned suppression technique"). Hutson and Masterton measured difference limina but progressively presenting smaller and smaller changes in air current frequency or amplitude. While their technique represents an elegant application of learning paradigm to animal psychophysics, there are some drawbacks regarding precision of stimulus application. For example, the rats are constantly licking off a water spout during stimulus application, and the associated head movements presumably cause enough whisker motion to considerably elevate detection and discrimination thresholds. Moreover, Hutson and Masterton could modulate the air current's frequency only up to 32 Hz, because the stimulation apparatus generated audible sounds above that frequency. For comparison, in studies on anesthetized animals, frequencies from 300-750 Hz are employed routinely (Arabzadeh et al., 2003; Andermann et al., 2004).

Zeigler and coworkers (Bermejo et al., 1996; Harvey et al., 2001) set a new standard for whisker-dependent behavioral tasks by making use of a head-fixed rat preparation. Harvey et al. presented one of two objects (a cube and a sphere) to one side of the rat's face, which was free to palpate the object with its whiskers. The rat was operantly conditioned to press a lever located next to its forepaw on a variable-ratio schedule on a go-no-go-task, with object identity as a discriminative stimulus signaling the opportunity to obtain a water reward. Their paradigm provides the unique opportunity to study active sensorimotor integration in the whisker system: the rat has to rely exclusively on its whiskers to sample the required information, but unlike in other paradigms, the discriminanda can be flexibly controlled and interchanged, and whisking trajectory of single whiskers can be conveniently monitored with optoelectronic devices at a very high spatiotemporal resolution.

These novel paradigms offer exciting prospects to study the rat whisker system, especially in the active whisking mode. Nonetheless, there exists a stark contrast between the coarseness of stimulus application characteristic for behavioral studies and the extremely high spatiotemporal precision of stimuli used for electrophysiological investigations in anesthetized animals. Here, several investigators have reported responses to whisker deflections of only several micrometers amplitude from first-order trigeminal ganglion (TG; Gibson & Welker, 1983) and also cortical neurons (Barth, 2003), together with a temporal precision of responses in the sub-millisecond range (Jones et al., 2004ab; Deschenes et al., 2003). Therefore, it seems highly demanded that psychophysical investigations of the whisker system employ stimuli with a spatiotemporal precision matching that resolution ? micrometer precision on a millisecond time scale. Designing such tasks is challenging due to the difficulty of applying spatiotemporally precise stimuli to awake behaving rats while at the same time precluding non-vibrissal stimulus sources (such as cutaneous receptors or the small perioral sinus hairs). Also, these constraints must be met under conditions

which allow for the assessment of psychophysical detection or discrimination curves, i.e. in the context of a well-controlled behavioral paradigm.

1.3 Psychophysics in the primate somatosensory system

Unlike psychophysics in the whisker system, psychophysics in the primate tactile system has a long and rich tradition, starting as early as the late 19th century (Treitel, 1897). Today, the primate tactile system is described as being composed of psychophysical "channels". Gescheider et al. (2002) define information processing channels in sensory systems as "elements that are tuned to specific regions of the energy spectrum to which the system responds". The channel concept has proven extremely useful in the investigation of sensory systems. For example, it allows to differentiate hypothetical subsystems proposed on the basis of psychophysical studies from neuronal subclasses identified physiologically. Moreover, it can serve to forecast structural or functional principles of the nervous system, such as Ewald Hering's theory of color-opponent channels anticipated the discovery of color-opponent cells in the retina and the lateral geniculate nucleus (Goldstein, 1997).

In touch, a continuous range of stimulation frequencies is sampled by three (monkey) or four (man) different channels with different frequency tuning curves. The first suggestion that the sense of touch might be served by at least two separate channels was based on a discontinuity in the detection threshold curve when moving from low to high-frequency stimuli (von Békésy, 1939). Further psychophysical experimentation was done to isolate the properties of the presumed subsystems. Verrillo (1963) measured psychophysical amplitude detection thresholds to vibratory stimuli applied on the fingertip as a function of frequency. He found that, when increasing the contactor area of the tactile stimulator, detection thresholds decreased markedly at high frequencies but remained unaffected at low frequencies. Aside from interpreting this finding as evidence that tactile vibratory sensation is mediated by at least two subsystems, he identified "spatial summation" as a property of the channel believed to mediate detection of high-frequency vibrations (later termed P). Shortly thereafter, Verrillo (1965) conducted another experiment, in which he manipulated the total duration of the vibratory stimulus. He found resultant threshold decreases at high but not low frequencies, and interpreted this observation to indicate another property of the P channel, namely "temporal summation". Subsequently, the P channel could be linked to the Pacinian corpuscle (Verrillo, 1966; Mountcastle et al., 1972) and the other channel (termed NP for "non-Pacinian") to Meissner's corpuscle and the quickly adapting fiber type (Talbot et al., 1968). The two channels were later joined by two additional ones, termed NP II (Capraro et al., 1979; Gescheider et al., 1985) and NP III (Bolanowski, Jr. et al., 1988). NP II could be aligned with Ruffini receptors and slowly adapting fibers of type II, while NP III could be aligned with Merkel receptors and slowly adapting fibers of type I (Bolanowski, Jr. et al., 1988). The four psychophysical channels described in humans have overlapping sensitivity

ranges. Accordingly, there are stimuli capable of activating all four channels simultaneously. Channels are assumed to interact in these situations, which is interpreted as an integration across channels occurring in the central nervous system (Gescheider et al., 2002; Gescheider et al., 2004).

1.4 Physiology of perception

While behavioral data on sensory channels is useful to constrain hypotheses regarding functional organization as well as guide research on sensory systems, it cannot, by itself, resolve all questions regarding their neural underpinnings. Thus, Ewald Hering's theory of color-opponent channels was seemingly at odds with the Young-Helmholtz theory of trichromatic color vision, until it was found that both theories yield valid descriptions of the visual system, but apply to different stations of the visual pathway (Goldstein, 1997).

One of the central topics in the literature on the physiology of perception is the question if and how the neuronal signals from sensory neurons at any stage of sensory pathways are combined to yield a percept (Barlow, 1972; Parker & Newsome, 1998). A related question is what mechanism limits the perceptual resolution of the senses, concerning both detection and discrimination of sensory signals.

The lower envelope principle (De Valois et al., 1967; Talbot et al., 1968; Barlow, 1972) asserts that detection and discrimination performance of an observer is limited by the most sensitive neural element available. Despite the audacity of this proposition, a considerable body of evidence has been summoned supporting this view. Sakitt (1972) showed that absorptions of a single quantum in the human retina results in a measurable perceptual effect, and took this to imply that observers can count single spikes or at least discrete bursts of action potentials in one critical sensory neuron. In the peripheral branch of the somatosensory system, psychometric detection thresholds of vibrotactile stimuli are a function of the most sensitive receptor class available at a given range of frequencies (Mountcastle et al., 1967; Mountcastle et al., 1972; Bolanowski, Jr. et al., 1988). Even within a given receptor class, very few individual fibers coupled to the given receptor class exhibited lower thresholds than animal or human observers. Moreover, it has been claimed that a single spike in a single rapidly adapting fiber suffices to elicit a percept (Johansson & Vallbo, 1979; Vallbo et al., 1984; Ochoa & Torebjork, 1983).

However, this picture is complicated by observations that, in some cases, even the most sensitive fibers can be considerably less sensitive than the observer. For example, Johnson et al. (1973) found that only a weakly correlated neuron pool of 50 thermoreceptive fibers was able to transmit enough information to account for psychophysically measured difference limina. Such results support a "response pooling" model of detection, in which psychophysical thresholds exceed that of the most sensitive elements in the neuron pool.

The inverse finding, that an observer is less sensitive than many of his individ-

ual neurons, has also been obtained. Britten et al. (1992) showed that about half of the single neurons recorded in visual area MT matched or outperformed monkey observers. Consequently, they built a response pooling model in which the psychophysical threshold is a function of a pool of weakly correlated neurons, in which the information carried by the most sensitive elements is partly obscured by that of less sensitive elements (Shadlen et al., 1996).

This discrepancy between findings supporting either the lower envelope model or some kind of response pooling model cannot be resolved by assigning one or the other to either the sensory periphery or the central nervous system, nor by assuming that one sensory modality exclusively follows one of the coding schemes. Thus, the response pooling approach of Britten et al. (1992) in visual area MT is at odds with the observations of Vogels & Orban (1990), who recorded in monkey V1 while the animals worked on an orientation-discrimination task, and found support for the lower envelope principle. In the somatosensory system, it has been proposed that a single spike in a single rapidly afferent fiber suffices for detection, while a larger number of spikes is required in single slowly adapting fibers (Vallbo et al., 1984; Ochoa & Torebjork, 1983). In monkey primary somatosensory cortex, detection thresholds of vibrotactile frequencies follow average neuronal sensitivity (de Lafuente & Romo, 2005), while discrimination thresholds of such stimuli are governed by the lower envelope principle (Hernandez et al., 2000). Lastly, Geisler & Albrecht (1997) compared behavioral thresholds for visual contrast and spatial frequency discrimination with thresholds of V1 neurons, finding evidence for a lower envelope model in monkeys but for response pooling in cats.

Taken together, both coding schemes seem to be at work, and neither species nor sensory modality nor central vs. peripheral location of neural elements suffices to predict the applicability of either coding scheme in a given subsystem or perceptual channel.

1.5 Aim and scope of this dissertation

Although the whisker-to-barrel pathway has served as a model system for sensory processing for decades (Petersen, 2003), there exists a gap between acute neurophysiological and behavioral studies. As outlined before, the highly precise stimulus kinematics employed in the former is contrasted by the coarse and uncontrolled stimuli used in the latter. To bridge this gap, I developed a novel method of assessing psychophysical detection thresholds in operantly conditioned, head-fixed rats. Unlike previous behavioral paradigms, this novel one allows for extremely precise whisker stimulation in awake rats, while, at the same time, behavioral responses can be recorded. Moreover, this preparation can easily be combined with neurophysiological recordings from chronically implanted electrodes. In this dissertation, I attempt to demonstrate the usefulness of the method by showing that behavioral data obtained through it lends itself to the generation of predictions concerning the structural and functional

organization of the rat whisker system.

So far, little experimental effort has been directed towards a characterization of the whisker system on a perceptual level. Accordingly, it is not known whether the system can be described as consisting of distinct psychophysical channels. To my knowledge, the first description of tactile channels dates back to Georg von Békésy (1939), who based this conclusion on a discontinuity in a psychophysical threshold curve, implying that the system behaves differently in two parts of the kinematic space. Similarly, I challenged the rats with a wide range of tactile stimuli to see whether the impact of any given kinematic parameter on stimulus detectability is affected when combining it with a range of values of another one.

Beyond the level of description attainable by behavioral experiments alone, the concurrent registration of behavioral and neuronal responses can provide the basis for correlating neuronal activity in sensory pathways and perceptual events. Such data is, at present, lacking for the whisker system; accordingly, coding mechanisms discussed in the literature on human or monkey psychophysics, such as the lower envelope principle or response pooling, have not yet been investigated. However, any successful model system for sensory processing will, at one point, have to provide means for assessing the relation of the two. To address this question and elucidate the relation of neuronal responses to perception, I combined the psychophysical detection task with unit recordings from barrel cortex.

2 Psychophysical detection task and recordings from the trigeminal ganglion

2.1 Chapter introduction

This chapter describes two experiments. The first one concerns the establishment and successful application of a head-fixed, behaving rat preparation that allows measuring detectability of a single whisker deflection as a function of stimulus kinematics. Although inspired by von Békésy's (1939) initial finding of a discontinuity in the threshold curves to vibrotactile stimuli, I opted to characterize the stimuli in terms of kinematics instead of frequencies. Describing tactile stimuli in frequency space has the disadvantage about being ambiguous with respect to kinematics; in principle, a given frequency can exhibit any conceivable amplitude, velocity, and acceleration. Theoretically, every frequency can be perceptually suprathreshold when the amplitude is very large (and therefore velocity and acceleration are, too) or subthreshold when the amplitude is very low. Moreover, it is not the frequency of a stimulus that drives the mechanoreceptor, but its kinematics (Johnson et al., 2000).

Using this novel method, I obtained data that indeed support the notion that the whisker system is comprised of at least two psychophysical channels. Thus, a second experiment was conducted to test the hypothesis that the two channels can be aligned with two well described classes of whisker primary afferents, the slowly and rapidly adapting neurons in the trigeminal ganglion.

2.2 Methods

All experimental and surgical procedures were carried out in accordance with standards of the Society of Neuroscience and the German Law for the Protection of Animals. Subjects were six (psychophysics) and nine (neurophysiology) male Sprague-Dawley rats (Harlan Winkelmann, Borchen, Germany), aged 12-16 weeks.

Surgery to implant the head mount

Anesthesia was introduced with a combination of ketamine and xylazine (100 mg/kg and 10 mg/kg body weight) injected i.p., and maintained with isoflurane (1-2 %). The rat was positioned in a stereotaxic apparatus, the skull was exposed and holes were drilled for placement of 11 stainless steel screws. Screws were embedded in dental cement (FLOWline, Heraeus Kulzer, Hanau, Germany). Additionally, a mounting screw turned upside down was placed in the head-cap. For EMG recordings, teflon-insulated silver wires (0.003" bare, 0.0055" coated; A-M Systems, Inc., Carlsborg, WA, USA) were inserted into the left whisker pad and soldered to a connector embedded in the head-cap. The wound was treated with antibiotic ointment and sutured. Analgesia and warmth was provided after surgery. Rats were allowed to recover for at least ten

days before habituation training commenced. Rats were housed individually and kept under a 12:12 light-dark cycle (lights on at 10 a.m.) with water and food available ad libitum except for the periods of water restriction. During the period of behavioral testing, the rats were water-restricted for five days per week. Drops in body weight, monitored daily, were prevented by supplementary water.

Whisker stimulation

Whisker stimulators were constructed from piezo actuators (Physik Instrumente, Karlsruhe, Germany). A thin glass capillary (Science Products GmbH, Hofheim, Germany) was glued to the actuator. The opening at the free end was reduced to a size of 225 μm with dental cement enveloping a small plastic tube which was taken out after hardening of the cement (Fig. 2.1a, inset).

Voltage commands were programmed in LabVIEW (National Instruments Corporation, Austin, TX, USA); each stimulus was composed of a fast half cosine wave followed by a 500 ms plateau and another half cosine wave at 0.5 Hz for a very slow return (Fig. 2.1b). The frequencies of the half cosine waves at stimulus onset were adjusted at each of five amplitudes to yield five different velocities. The range of kinematic parameters covered were 110 μm to 1100 μm for amplitude, and 5.4 mm/s to 130.9 mm/s for velocity. These values correspond to 1° to 12°, and 62 °/s to 1500 °/s if applied 5 mm from the whisker base, respectively.

The stimulators were calibrated at the outset of the study with a modified phototransistor sampled at 50 kHz with 1 μm precision (H21A1, Fairchild Semiconductor Corporation, South Portland, ME, USA), and an optoelectronic measurement device (laser emitter and detector, resolution 1.4 ms, 11 μm; PAS 11 MH; Hama Laboratories, Redwood City, CA, USA).

Three of 47 stimuli displayed some ringing following stimulus offset at a maximum peak-to-peak amplitude of 7 μm ($< 0.1°$). Importantly, the peak velocity of the after-oscillations did not exceed 20 mm/s (230 °/s) for any of the three stimuli while clear signs of detectability at these amplitudes were visible only if the peak velocity exceeded two to three times this value (with non-ringing stimuli). Fig. 2.1c shows two exemplary calibration traces, the smaller of which displays the stimulus with the largest after-oscillations used in this study.

To ensure precise whisker stimulation, the relative position of the stimulator to the rat's snout was monitored via a video camera from above, and a picture was taken before each individual session (Fig. 2.1a). Using a 5 mm comparison snippet attached to the glass capillary, the distance of the capillary tip to the base of the whisker was adjusted to 5 mm with a precision of +/- 1 mm. To ensure that the stimulator immediately engaged the whisker at stimulus onset, the capillary and the whisker were tilted against each other at an angle between 155° to 175° such that the vibrissa rested against the inside wall of the capillary (Fig. 2.1a). Furthermore, care was taken to stimulate the whisker in its null position, i.e. at resting angle relative

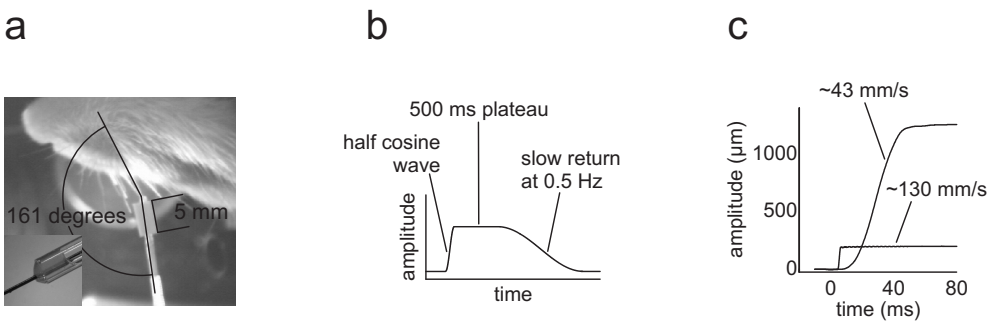

Figure 2.1: Method for precise stimulus application. a) Rat and whisker stimulator viewed from above to illustrate measurements of the distance of the capillary tip to the base of the whisker and the angle between capillary and whisker. Inset: close-up to show the point of insertion of the whisker into the narrowed opening of the capillary tip. b) Illustration of stimulus construction. c) Calibration traces of two exemplary stimuli with medium (43 mm/s) and high 130 mm/s) peak velocities. The amplitude of ringing after the high velocity deflection trace is the highest observed in the stimulus set used in this study.

to the face.

Experimental setup

To allow for precise whisker stimulation without contamination of body and head movements, the rat was placed in a restraining box, and the head was fixed using the mounting screw to a metal bracket above the exit of the restraining box (Welsh, 1998). The restraining box was put inside an experimental chamber with light- and sound-absorbing enclosing. A spout was positioned in front of the rat's snout for water delivery. To the left of the animal's head, a moveable laboratory-built metallic arm was mounted, holding the whisker stimulator. At the beginning of each training session, the whisker C1 was attached to the stimulator. Deflections were always in the rostral-to-caudal direction. Licking movements were detected using the interruption of an infrared beam by tongue protrusion. The rat was constantly monitored using an infrared-light sensitive camera mounted inside the experimental chamber. EMG recordings were done using an extracellular amplifier (MultiChannelSystems, Reutlingen, Germany) at a sampling frequency of 5 kHz. Voltage traces were digitally full-wave rectified and low-pass filtered (10 Hz) offline to yield an envelope trace.

Behavioral task

Rats were habituated to the experimental situation by subjecting them to a systematic desensitization procedure for two to three weeks after which all animals tolerated head-fixation without any sign of stress. They were then put on water restriction and conditioning commenced. Initially, animals were trained to lick on a fixed-interval schedule of initially 0.5 s that was incremented step-wise to 5 s. Next, a well detectable

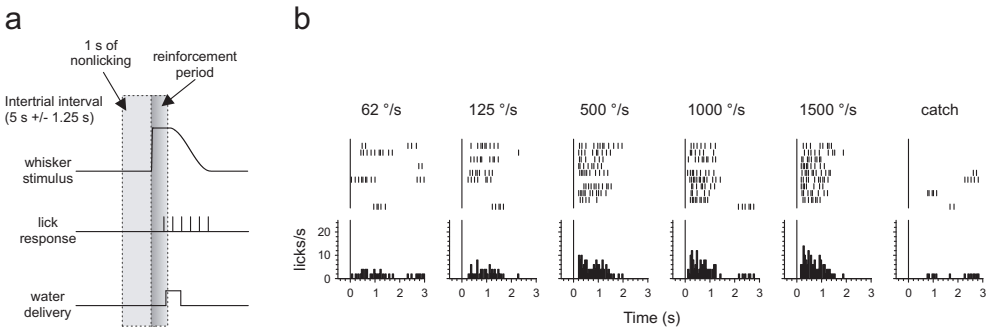

Figure 2.2: The psychophysical paradigm. a) Illustration of the psychophysical paradigm. b) Licking behavior during a single session. Each tick in the raster plot indicates a lick at the water spout. Peri-stimulus time histograms below show overall responses to a given stimulus. In this session, five different types of whisker deflections (same amplitude (12°), differing velocities) were presented plus a catch trial in which no stimulus was presented and licking was not reinforced.

rectangular deflection applied to a single whisker served as the discriminative stimulus and occurred every 5 s +/- 1.25 s. The first lick emitted within 500 ms after its onset (reinforcement period, gray field in Fig. 2.2a) yielded water reinforcement. To discourage random licking during the intertrial interval, a period of 1 s without licking was required before a new stimulus would be delivered. In case the animal licked during that period, the scheduled delivery of the next stimulus was delayed by 1 s. Once the rat would emit lick response at a short latency (< 500 ms) to the rectangular deflection in 90 % of traces, psychophysical testing began.

Psychophysical testing was conducted employing the method of constant stimuli. In one session, four to ten stimuli of identical amplitude but differing peak velocities were presented in pseudo-random order, each of them for ten times. In addition, a "catch" stimulus was included, in which no deflection of the whisker occurred, but lick responses in a time window of 500 ms were recorded to yield a measure of chance performance. Over the entire course of the experiment, each stimulus type was presented to the rat at least 50 times. To avoid frustration of the rat confronted with many sub-threshold stimuli, easily detectable reference stimuli (medium-amplitude pulses) were interspersed with the stimuli of interest. The response to these stimuli also served to monitor the overall performance of the animal. Sessions in which responses to the reference stimulus were below 70 % were not included into the sample. To ensure that rats responded to tactile input only, white noise (˜ 80 dB) was presented during sessions. Moreover, none of the animals responded consistently in control sessions that were identical to experimental sessions, except that the whisker was detached from the stimulator, assuring that non-vibrissal cues did not play a role for their performance.

Electrophysiological recordings

Rats were anesthetized as described above and placed in a stereotaxic frame. A craniotomy was performed to expose the right cerebral hemisphere, which was then gently aspirated to visualize the trigeminal ganglion at the base of the skull. After careful hemostasis, the dura overlying the ganglion was teased away, and laboratory-built pulled and ground glass-coated platinum tungsten electrodes (80 μm shank diameter, 23 μm diameter of the metal core, free tip length ˜ 8 μm, impedance: 3-6 M?; Thomas Recording, Giessen, Germany) were lowered until units responding to manual whisker stimulation were encountered. Band-pass filtered (300-10,000 Hz) voltage traces were recorded at 20 kHz sampling rate using an extracellular amplifier (MultiChannelSystems, Reutlingen, Germany). At the end of the experiment, the rat was killed with an overdose of pentobarbital.

Selection of units and analyses

Once a unit with sufficient spike amplitude was isolated, the receptive field characteristics (responsive whisker and directional preference) was assessed using a hand-held rod. As reported earlier (Lichtenstein et al., 1990), slowly adapting units (see below for classification) often showed directional preference. Only those units that exhibited a strong response for horizontal rostro-caudal stimulus directions were included in the sample. After attaching the piezo bender to the responsive whisker in the same fashion as done in the awake animals, a subset of the whisker deflection stimuli used in the psychophysical experiments was applied. This subset included five of the six stimulus amplitudes (1, 2, 4, 8, 12°) and five of the seven peak velocities (62, 250, 500, 1000, 1500 °/s), yielding a total of 25 different stimuli. Ten presentations per stimulus were presented in pseudorandom order at an interstimulus interval of 1.5 s.

All analyses were done offline. First, stimulation artifacts and occasional multi-unit activity was sorted out by an automated spike-sorting algorithm (Hermle et al., 2004). Sorting results were checked by the experimenter by visually comparing spike trains with raw traces. Only clear single unit spike trains entered the present data set. Then units were classified as slowly adapting (SA) if activity to a fast, high-amplitude deflection (12°, 1500 °/s) was sustained longer than 25 ms after stimulus onset. Alternatively, in case the neuron was quiescent at this time, it was classified as rapidly adapting (RA). Because SA neurons are known to occasionally display phasic responses to some directions of deflection (Lichtenstein et al., 1990), the possibility that SA cells could erroneously be included into the RA group had to be considered. We, therefore, manually checked whether the cell responded tonically to other directions of deflection and did not include it as RA in case it did. Second, response parameters across the stimulus set of cells classified here as RA were very homogenous and well separated from those that classified here as SA (see results section). This fact validates the classification criterion. For instance, in the parametric range in

which SA usually show phasic responses (low velocities), the spike count of SA cells was well separated from the ones of the RA group. The latter generated a maximum of 1.2 spikes/stimulus in response to high amplitude stimuli of the lowest velocity while the same stimulus with no exception triggered more than 4.6 spikes/stimulus in cells within the SA group. Another example is the fact that none of the presumed RA cells displayed any obvious modulation by change of amplitudes while each and every cell classified as SA did. In summary, RA pool contamination with SA cells can be excluded with high probability.

The peri-stimulus time histogram (PSTH) was calculated as spike renewal function using a bin width of 0.1 ms and integration window of 1 ms (Abeles, 1982). For RA units, spike counts per stimulus were determined by integrating the PSTH from 0 to 250 ms post-stimulus time. For SA responses, the first step was to determine the time of maximal firing rate during the transient response using the PSTH smoothed with a moving Gaussian (50 bins). Integration windows of different length were centered at the time of maximum firing rate and the spikes were counted by integration of the non-filtered PSTH in this window.

Statistics

Response probability of a single subject was calculated as the mean response rate from at least five sessions employing a given stimulus type. Statistical comparisons of behavior group data were made using the nonparametric Friedman test. The principal range of kinematic parameters tested was 1° to 12° amplitude and 62 °/s to 1500 °/s velocity. While not all of the six rats were confronted with the full stimulus set for practical reasons, and since I employed a related-samples test for higher statistical power, statistical comparisons are not based on all six animals, but on three to four depending on parameter set. In spite of the low power inherent in small-sample studies, effect sizes were so large that the small sample size did not pose a major constraint. In addition, data from the four animals in which most of the parametric range was explored were analyzed on an individual basis using the nonparametric Kruskal-Wallis test. Since the main trends reported here were identical for all animals, Figs. 2.3bc shows data from all six rats. Plots depict mean response probabilities, error bars represent standard error of the mean (SEM). Neurophysiological data with number of spikes or peak firing rate as dependent variables were analyzed with 2-way analyses of variance with amplitude (five levels) and velocity (five levels) as factors. In addition to p-values, standardized effect sizes (?2) are given. ?2 varies between 0 and 1 and represents the amount of explained variance by a given factor or by their interaction. To disentangle the roles of velocity and acceleration in the neurophysiological data, multiple regression analyses with two to three independent variables were computed (combinations of amplitude, velocity, and acceleration). The square of the multiple correlation coefficient, R2, reflects the amount of variance explained by the independent variables. Semipartial correlations reveal the correlation

of an independent and a dependent variable in the equation when the correlation of the independent with another independent is controlled for. Again, its square (r2) indicates the amount of explained variance. All calculations were done in MATLAB 7.0 (The MathWorks, Natic, MA, USA).

2.3 Results

General observations

Lick responses recorded during a typical behavioral session are depicted in Fig. 2.2b. The probability to emit licks increased with increasing stimulus peak velocity. After training, all animals broke the light beam at latencies of ˜ 250 ms to well detectable stimuli. In the over-trained state of the animals, at which the psychophysical testing was performed, whisker movements rarely occurred. If they did, the movements were of low amplitude and short duration. Large amplitude rhythmic whisking ? characteristic for exploration ? was never observed. EMG activity of the whisker pad recorded in one animal confirmed this impression (data not shown). The fact that head-fixed rats dramatically decrease whisking activity ? if not explicitly reinforced for whisker movements ? has been reported by other investigators (Gao et al., 2003). Mean catch trial performance ranged between 12 % and 18 % and does not differ between sets (p = 0.881, data not shown).

Psychophysics

Mean response probability for one example subject is shown in Fig. 2.3a (velocities from 62 °/s to 250 °/s have been omitted for clarity in Figs. 2.3ab but are contained in the statistical analysis). Each line represents an "isovelocity set" of stimuli, i.e. stimuli in which the peak velocity remained constant. The four curves overlap at 4°, 8°, and 12°, but characteristically dissociate at smaller amplitudes (gray shaded area). This phenomenon is also visible in group data (Fig. 2.3b). Comparisons across amplitudes for isovelocity sets of medium velocities indicate better performance at higher amplitudes (Fig. 2.3b, 250, 500, 750, and 1000 °/s; p = 0.017, p = 0.012, p = 0.017, p = 0.059, respectively). Detectability at the extremes of peak velocities tested showed rather constant performance ? either high with high velocities (Fig. 2.3b; 1500 °/s: p = 0.355) or low with low velocities (62 °/s, 125 °/s: p = 0.399, p = 0.21, respectively, data not shown in Figs. 2.3ab). Thus, while amplitude of whisker deflection determines detectability at medium velocities, it seems insufficient for detection when peak velocity is low (< 250 °/s) and irrelevant when peak velocity is high (1500 °/s).

Next, we concentrate on the trajectories of the curves with peak velocities between 500 and 1500 °/s. It is obvious from Figs. 2.3ab that detection curves obtained with different isovelocity stimulus sets behave in a bimodal manner dependent on the amplitude. At low amplitudes (1° to 3°, gray shaded area in Figs. 2.3ab) peak velocity

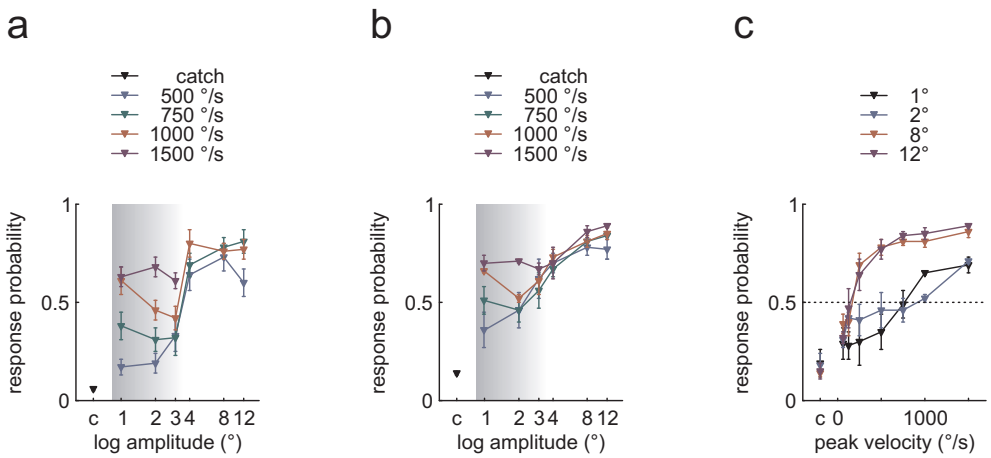

Figure 2.3: Psychophysical performance. a) Mean response probability +/- standard error of the mean (SEM) for one example animal. Curves represent isovelocity sets, varying in amplitude. Velocities from 62 °/s to 250 °/s are omitted for clarity. Shaded area highlights amplitude range in which peak velocity had a significant effect in determining the detection probability. b) Same as a), but averages across data from four animals. c) Mean response probability +/- SEM for four animals. Curves represent isoamplitude stimulus sets, varying in peak velocity. Dotted line indicates 50 % performance.

matters because the detection curves largely diverge. In contrast, the curves follow virtually the same trajectories for higher amplitudes indicating no contribution of peak velocity to detection in this range. Accordingly, response probabilities for peak velocities at 500 °/s to 1500 °/s (Fig. 2.3b) differ at small amplitudes (1°: $p = 0.029$, 2°: $p = 0.058$) but not at larger amplitudes (3°: $p = 0.308$, 4°: $p = 0.284$, 8°: $p = 0.758$, 12°: $p = 0.392$). Thus, peak velocity contributes differently to detectability at small vs. large whisker deflections. In Figs. 2.3ab, not all peak velocities have been included for illustration purposes.

Therefore the low velocity threshold at large amplitudes was not captured. This can be more easily appreciated if the detection curves are plotted across peak velocity (Fig. 2.3c). Depicted in this way, the curves correspond to "isoamplitude sets" of stimuli and directly depict the contribution of peak velocity to detection probability (amplitude sets close to the border of the two ranges, 3° and 4°, are omitted because interindividual variability of this border did not permit a clear picture). While both the low-amplitude curves and the high-amplitude curves increase with peak velocity (1°: $p = 0.012$, 2°: $p = 0.012$, 8°: $p = 0.009$, 12°: $p = 0.009$), the point at which detection probability reaches 0.5 (from here on referred to as "velocity threshold") clearly differs (˜ 125 °/s for large amplitude, ˜ 750 °/s for small amplitudes).

In summary, I found that a stimulus amplitude of ˜ 3° divided detectability into two qualitatively different modes. Small stimuli ($< 3°$) were detected only at high peak velocities (˜ 750 °/s) while large stimuli ($> 3°$) were detected at substantially

lower peak velocities (˜ 125 °/s; Fig. 2.3c). Thus, I suggest the existence of two psychophysical channels defined by both amplitude and velocity. The first channel (W1) responds to large amplitude and slow velocities, while the second channel (W2) responds already to small amplitudes but requires higher peak velocities (gray area in Figs. 2.3ab). As estimated from Figs. 2.3bc, the threshold activation for W1 would be ˜ 3° and ˜ 125 °/s while the threshold for W2 is $< 1°$ (not assessed by the present stimulus range) and ˜ 750 °/s.

This pattern of results for aggregated data was closely matched in analyses of individual performance data. The performance of all animals increased significantly as a function of velocity at each tested amplitude from 1-12° (all p's < 0.05). Performance curves for isoamplitude sets were statistically distinguishable between large (8° and 12°) and small (1° and 2°) amplitudes (8° and 12° vs. 1° and 2°; all p's < 0.05) but not within either large or small amplitudes (1° vs. 2° and 8° vs. 12°; all p's > 0.4). Thus, both group and individual data support the notion of two different sensitivity ranges.

Trigeminal ganglion recordings

Next, I tested whether the two proposed psychophysical channels can be assigned to the well described neuronal classes of SA and RA primary afferents in TG. Known response profiles of TG cells to stimuli similar to mine (Shoykhet et al., 2000) led me to hypothesize that W1 is based on SA, and W2 on RA primary afferents. However, the neurometric curves by Shoykhet et al. covered only about a third of the amplitude range covered here (them: 2.5° to 6°, me: 1° to 12°) and did not report an amplitude threshold for SA cells. Moreover, these authors used very high velocities (minimum of 1000 °/s) that were suprathreshold at all amplitudes tested here (in the present dataset, the velocity range extended from 62 °/s to 1500 °/s). Therefore, their data set was not sufficient to confirm or disprove alignment of the proposed channels with RA and SA cells.

Single unit data in anesthetized animals were assessed while stimulating a whisker in identical fashion as in the psychophysical experiments. The total sample in this study comprises 57 single units of which 14 were classified as SA, and 43 as RA. Of the RA units, 16 responded to a wide range of stimuli contained in the stimulus set; they were used to extract the neurometric data presented below. The remaining 27 RA units exclusively responded to step-like deflections (exhibiting highest velocities, but not usable to extract precise kinematic parameters due to mechanical limitations) and were not further analyzed.

Fig. 2.4 shows typical responses of RA and SA units to a high isoamplitude stimulus set (12°). RA cells gave responses to stimuli at higher peak velocities but only rarely to stimuli at lower peak velocities (Fig. 2.4a). Uniformly, the response profile was a fast transient (consisting of one to six spikes maximally lasting to 22.5 ms after stimulus onset). Applying the same stimuli, SA units already responded at

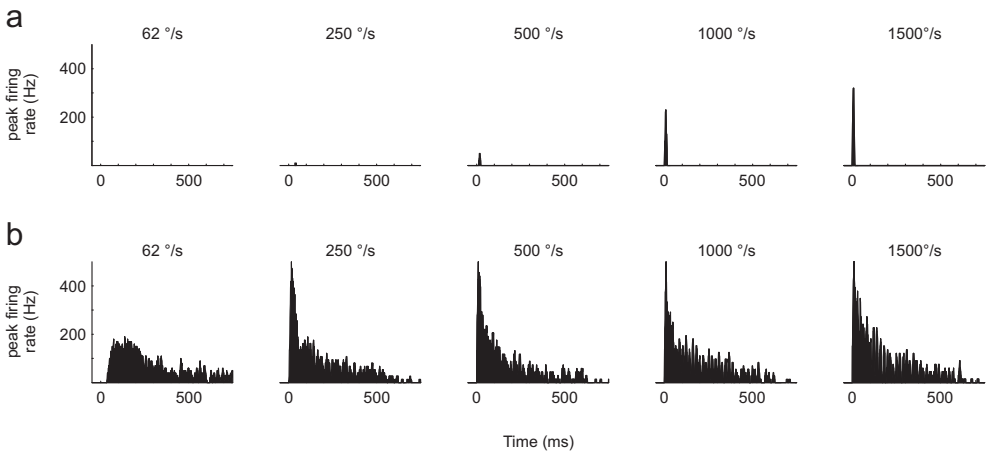

Figure 2.4: Typical peri-stimulus time histograms (PSTH) of trigeminal ganglion (TG) neurons. a) Rapidly adapting TG neuron (RA). b) Slowly adapting TG neuron (SA). Both PSTHs were constructed from ten presentations of a large-amplitude (12°) stimulus at five different velocities.

lower peak velocities with clearly discernible phasic and tonic responses (Fig. 2.4b). Typically, the phasic response increased with increasing peak velocity in contrast to the tonic portion that was expressed in a more uniform way across different peak velocities.

Plotting the number of post-stimulus spikes generated by RA units across the entire stimulus set, fully confirmed the prediction drawn from the characteristics of W2. RA activity increases as a function of velocity (F = 51.8, df = 4, p = 2.3*10-34, ?2 = 0.37) but not amplitude (F = 1.85, df = 4, p = 0.12, ?2 = 0.02) or their interaction (F = 0.76, df = 16, p = 0.74, ?2 = 0.03). Furthermore, robust RA activity (> 0.5 spikes/stimulus) is present only at velocities higher than 500 °/s, as observed with W2, and this holds regardless of amplitude (Figs. 2.5ab).

My first approach to measure SA activity was analogous to the one employed with RA cells. However, spike counts (that included the tonic response phase) yielded a less reassuring reflection of my predictions, in this case drawn from W1. SA spike counts readily captured the amplitude threshold typical of W1 ? they showed a sharp increase with amplitudes 4° or higher. Accordingly, SA spike count increased as a function of amplitude (F = 39.3, df = 4, p = 2.2*10-26, ?2 = 0.35) but not velocity (F = 0.13, df = 4, p = 0.973, ?2 < 0.01) or their interaction (F = 0.08, df = 16, p = 1, ?2 < 0.01). However, the measure completely failed to reflect the velocity threshold at around 125°/s which was characteristic of rats' detection probability in this parameter range (Figs. 2.6ab, compare to Fig. 2.3c).

In search for an alternative approach to fit the SA responses to the psychometric curve, it was found that maximal firing rates obtained from the transient phase in smoothed PSTHs yielded a near perfect match (data not shown). In order to arrive at

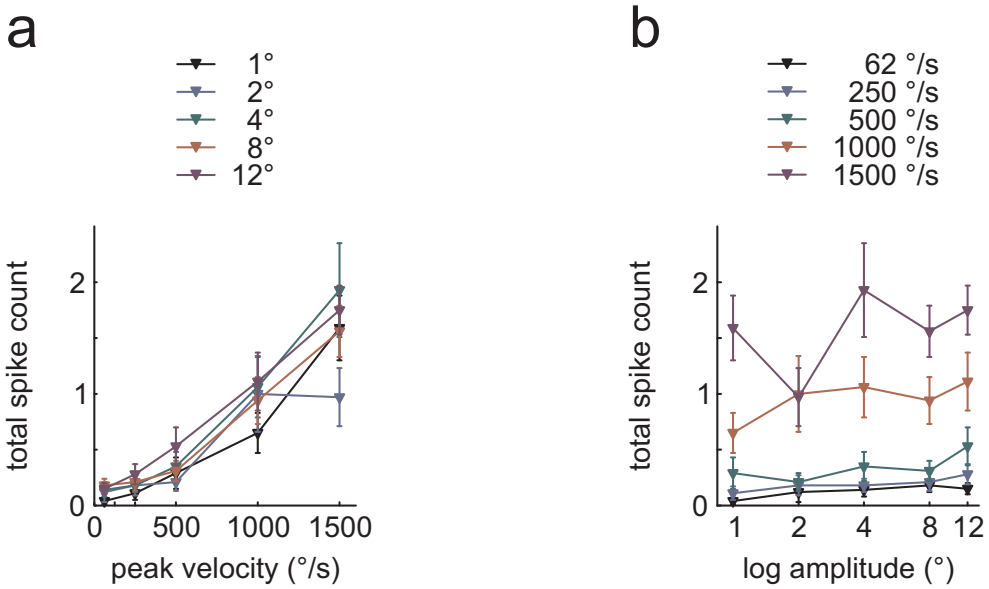

Figure 2.5: Neurometric plots of RA population responses (total spike count within 250 ms after stimulus onset) as function of peak velocity (a, curves represent isoamplitude sets) and amplitude (b, curves represent isovelocity sets). All graphs plot means +/- SEM.

spike counts as unit of measurement one has to find the optimal width of the window in which to integrate the PSTH. To this end, the unfiltered PSTH was integrated in windows of varying length which were centered on the time of maximum firing rate (as found in smoothed PSTHs). Next, the correlation of SA spike count and detection probability (in W1; i.e. using the means of responses to 8° and 12° stimulus amplitude) was calculated and the coefficient of determination (r2) was plotted against the width of the integration window. It turned out that windows of 2.8 ms to 13.2 ms length yield neurometric curves that explain > 95 % of the variance of the psychometric data (Fig. 2.6d). On either side of this optimal range the fit worsened steeply. Fig. 2.6c shows the resulting neurometric plots for one integration window below (1 ms), two inside (3 ms and 10 ms) , and one above (70 ms) the optimal range. In summary, the neurometric curve based on the transient SA response predicted the psychometric curve much better than the neurometric curve based on the total response dominated by the tonic portion. I therefore suggest that detection based on SA responses relies on very few spikes, generated during the transient response, rather than integrating spikes within long intervals.

To further illustrate the correspondence of psychometric and neurometric data in the parametric ranges spanned by W1 and W2, Fig. 2.7 plots SA responses well contained within the W1 range (mean peak firing rates with 8° and 12° amplitudes across all peak velocities) and RA responses well contained within the W2 range (mean spike counts with 1° and 2° amplitudes across all peak velocities) together with detection

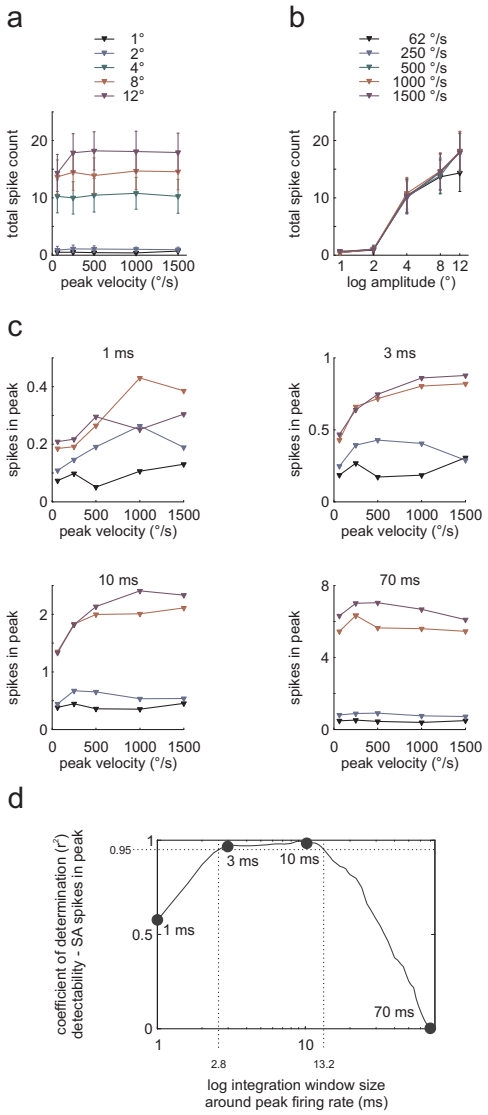

Figure 2.6: Neurometric plots of SA population responses. a and b: Total spike count within 250 ms after stimulus onset as function of peak velocity (a, curves represent iso-amplitude sets; means +/- 1 SEM), and amplitude (b, curves represent isovelocity sets; both graphs plot means +/- SEM). c) Isoamplitude sets (color code as in panel a) showing number of spikes in a window around peak firing rate of the transient response as a function of peak velocity. The four panels show results for four different integration window sizes (1, 3, 10, 70 ms). d) Coefficient of determination (variance in detection probability explained by SA spikes counts) as a function of integration window size. Gray dots indicate the corresponding example plots in panel c). The dotted line demarcates the range of window sizes in which > 95 % of the variance of the W1 curve were explained by SA peak spike count.

probability. The near perfect match of psychophysical and neurometric data strongly suggest that detectability in W1 is predominantly determined by SA responses while in W2 it is mainly based on RA responses. It is further noteworthy that the spike counts associated with threshold performance (0.5 detection probability) are low and quite comparable for SA and RA units (SA: 1.8 spikes at integration width of 9.2 ms as shown in Fig. 2.7 but 0.7 spikes at 3 ms, the lower end of optimal integration widths; RA: 0.7 spikes).

Coding of kinematic parameters in the whisker system

An obvious question is which kinematic parameter determines the detectability of whisker deflection. The stimuli used here contain sets of stimuli that potentially disentangle peak velocity and acceleration (isovelocity sets). However, the discontinuity of detectability around 3° and the suggested existence of two channels render this approach problematic as the question of coding has to be asked in the restricted parametric ranges that activate one channel but not the other. Unfortunately, due to technical reasons the amplitude range is limited in the present set of stimuli, most severely so for the important range of small amplitude, fast stimuli (W2, see methods section). It turned out that with behavioral data based on these restricted parametric ranges, the problem can not be resolved. A possible solution, however, is the availability of neurometric data from RA and SA cells across the entire amplitude range. The evidence, presented above, that these separable neuronal responses underpin the two channels, opens the possibility to address the question of coding of kinematic parameters by looking at the neurometric data of each class of primary afferents. RA spike count correlates positively with both peak velocity and acceleration with the first being a clearly better predictor of spike counts (r2vel = 0.35; r2accel = 0.08). Since peak velocity and acceleration do not show a fixed relationship within the set of stimuli used here, one can disentangle their relative contribution using semipartial correlations in the context of multiple regression (recall that the stimuli were designed to allow independent variation of these kinematic parameters by manipulating amplitude accordingly, i.e. there exist stimulus sets in which peak velocity is kept constant while peak acceleration varies). Using both kinematic parameters as predictors of RA spike count, a rather strong multiple correlation resulted (R2 = 0.36). Semipartial correlations revealed a substantial independent contribution of peak velocity (r2 = 0.29) but none for peak acceleration (r2 = 0.01), a strong indication that RA cells code for peak velocity, but do not reflect peak acceleration. For SA spike counts I only considered the measurements extracted from the transient response because the total spike count did not match the psychophysical data. Using an integration width of 9.2 ms , the semipartial correlations were r2 = 0.14 for amplitude, r2 = 0.09 for velocity, and r2 $<$ 0.01 for acceleration. In summary, peak velocity rather than peak acceleration determines the spike counts of RA and SA that are related closest to the detectability of whisker deflection.

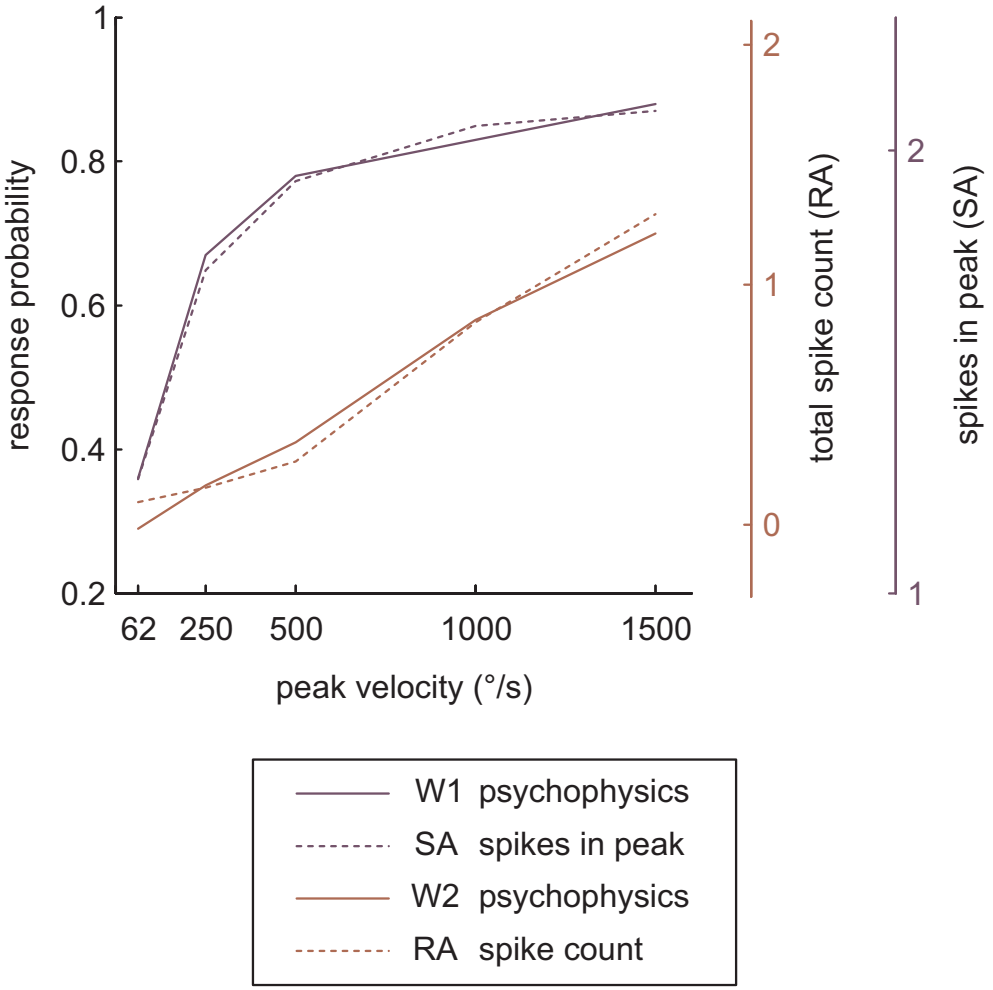

Figure 2.7: Overlay of psychometric and neurometric curves. Psychometrics: mean response probabilities for W1 (average of 8° and 12°, magenta) and W2 (average of 1° and 2°, red) as a function of peak velocity (left ordinate). Neurometrics: peak spike count SA population in W1 range (average of 8° and 12°, 2nd right ordinate, magenta), spike count of RA population in W2 range (average of 1° and 2°, 1st right ordinate, red). Peak spike counts for SA cells was calculated with an integration window size of 9.2 ms, in which the coefficient of determination reached its maximum (cf. Fig. 2.6d). Psychometric and neurometric curves show very similar trajectories (cf. Figs. 2.3 to 2.6). In order to allow the direct comparison of axes values, the scaling (translation and expansion) was done as to match the curves optimally.

2.4 Chapter discussion

How does neuronal activity give rise to perception? A sufficient answer to this question requires that the transformations from physically precise stimuli to specific neuronal activity, and finally to central representations that give rise to the percept are known. While the rat whisker system lets us study the transformations from stimuli to central representation in minute detail on the level of molecules, neurons and highly defined microcircuits, the relationship to perception has been elusive. The psychophysical paradigm described in this chapter complements the whisker model system by relating specific perceptual capabilities to neuronal activity.

Psychophysical properties of whisker stimulation in rats have been assessed early on (Vincent, 1912; Schiffman et al., 1970). It has been shown that rats are capable of amazingly fine discriminations of surfaces (Guic-Robles et al., 1989; Carvell & Simons, 1990) and apertures (Krupa et al., 2001), and that discrimination of textures and object forms are optimized by active scanning movements (Prigg et al., 2002; Carvell & Simons, 1995; Harvey et al., 2001). Finally, the detectability of 1° to 3° whisker deflections applied by a sinusoidally modulated air stream (at 0.1 to 32 Hz) in mobile rats was demonstrated in the only study so far that attempted to employ parameterized whisker deflections (Hutson & Masterton, 1986). However, none of these studies achieved the precision of stimulus control that is needed to causally relate physical properties of the stimulus to neuronal activity and to the percept. Optimal stimulus control becomes possible by taking advantage from a head restraint preparation (Hentschke et al., 2006) that allows to apply stimuli 5 mm from the face using a piezo bender in a highly controlled way ? a device that has been a standard for precise whisker stimulation in acute experiments for decades (Simons, 1983).

The whisker system uses two psychophysical channels

Based on the psychometric curves, the two-dimensional parametric space could be subdivided into 4 subregions delineated by an amplitude of ˜ 3° and a velocity of ˜ 750 °/s. Below 3°, only peak velocities $>$ 750 °/s could be detected consistently (W2), while above 3°, peak velocities $<$ 750 °/s (down to 125 °/s) were sufficient for detection (W1). In the two remaining parametric subspaces, detection probability was either very low ($<$ 3°, $<$ 750 °/s) or consistently high ($>$ 3°, $>$ 750 °/s). Detailed comparison of the psychometric curves with neurometric data from primary afferents in the TG, revealed a near perfect match of SA activity to detectability in W1, while RA activity matched the detectability in W2, yielding the first demonstration of two independent psychophysical channels in the rat whisker system. It should be noted, however, that additional channels might exist that were not detected in the present study, either because they were masked by more sensitive ones, or are responsive outside the tested parameter range as discussed above. Such additional channels may for example serve to monitor relative whisker position during a muscle-driven whisker

stroke (Szwed et al., 2003), directionality of deflection (Lichtenstein et al., 1990), or forces parallel to the hair shaft (Zucker & Welker, 1969).

Several studies suggest that in humans, SA fibers of type I (coupled to Merkel cell receptors), unlike RA afferents, which seem to follow the lower envelope principle, require a higher number of spikes to elicit a sensation (Talbot et al., 1968; Ochoa & Torebjork, 1983; Vallbo et al., 1984). The present results suggest a similar coding strategy in the rat whisker system. It was found that the close match between psychometric and neurometric curves (Fig. 2.7) was achieved only if transient rather than sustained portions of SA responses were considered. Inclusion of the tonic response portion of SA cells into the neurometric measure not only failed to improve the match with psychophysics, but rather seriously deteriorated it (cf. Fig. 2.6). Thus, very few spikes in a narrow time window between ˜ 3 ms to 10 ms may elicit a sensation. This implies that those central instances of the somatosensory system that give rise to the animals' percept may not receive (or use) the tonic portion of SA response. Supporting this notion, it has been found that SA encode dynamic kinematic parameters at a high temporal precision (Jones et al., 2004ab). Moreover, inhibitory mechanisms and/or synaptic depression at higher stages of signal processing lead to high-pass filtering of cortical tactile signals (Carvell & Simons, 1988; Swadlow, 1995; Chung et al., 2002; Ahissar et al., 2000; Moore & Nelson, 1998; Zhu & Connors, 1999), and responses in barrel cortex were observed to reflect the initial timing of thalamic afferent input rather than the total number of spikes (Pinto et al., 2000). In many natural contexts the availability of sensory stimuli is short and there is pressure to initiate behavioral decisions in a limited time span (Johansson & Birznieks, 2004). Presumably, such constraints have helped to evolve strategies applied by many sensory systems to extract relevant information from fairly low numbers of spikes (reviewed in Rieke et al., 1997). The temporal characteristics of the short non-repetitive tactile stimuli as used here fall into this class ? but it has to be borne in mind that coding strategies may be task or situation dependent and may differ for stimuli that are immanently stretched over time (Luna et al., 2005).

Channel separability downstream the trigeminal ganglion

Taking the suggested similarity of the rat whisker and the primate tactile systems one step further, one might speculate that columns in barrel cortex existed which receive differential input from either RA and SA units. The seminal paper of (Powell & Mountcastle, 1959) described such columns in monkey primary somatosensory cortex subarea 3b. The existence of such columns was later confirmed by several other investigators in several species of monkeys as well as in cats (Paul et al., 1972; Sur et al., 1981; Sur et al., 1984; Sretavan & Dykes, 1983).

But even though the notion of columnar organization of RA and SA units in primate somatosensory cortex has achieved textbook status (Kandel et al., 2000), this issue may not be fully resolved. A severe shortcoming of the above cited studies

was their mode of tactile stimulation; segregation of RA and SA cells was based exclusively on the presence or absence of a tonic response component to a ramp-and-hold skin indentation. Importantly, this does not exclude the possibility that part of the observed units with RA profiles were in fact driven by SA peripheral fibers, with the tonic component simply filtered out (as occurs in the rat whisker system; see chapter 3). Furthermore, these studies did not address the possible mapping of the other two mechanoreceptive fiber types, SA II and PC, even though cortical correlates of the latter were described much earlier (Mountcastle et al., 1969).

More recent attempts to clarify these issues employed sinusoidal rather than trapezoidal indentations, with frequencies and amplitudes tailored to isolate the three fiber subtypes SA I, RA, and PC, mediating the sensations of pressure (1 Hz), flutter (30 Hz), and vibration (200 Hz), respectively (Chen et al., 2001; Friedman et al., 2004). Under pentothal anesthesia, activation patterns observed with intrinsic optical imaging in area 3b of the squirrel monkey coincided; however, under isoflurane anesthesia, activation patterns revealed small (˜ 250 μm) patches of cortex that were preferentially (though by far not exclusively) activated by one of the three stimulus types (Chen et al., 2001). In addition, these patches hardly resembled the "bands" of alternating RA and SA units described e.g. by Sur et al. (1981, 1984). To sum up, while there is evidence for some anatomical segregation of projection zones of different fiber types, the exact amount and topography remains unclear.

Accordingly, it is difficult to derive predictions for a possible segregation of projection zones of RA and SA units in rat barrel cortex. In fact, no such segregation has been described so far. Similarly, it is unclear whether the easy separability of RA and SA cells at the level of the ganglion is preserved at stations of the whisker-to-barrel pathway located intermediate to ganglion and cortex. While there is some evidence that RAs and SAs are still kept separate functionally, perhaps even anatomically, in the trigeminal brainstem complex (Shipley, 1974), direct evidence for separability in VPM thalamus or barrel cortex is lacking. Most studies find no tonic response component of cortical units to ramp-and-hold whisker deflections (e.g. Simons & Carvell, 1989; Pinto et al., 2000; Webber & Stanley, 2004). The studies that reported tonic responses were conducted in urethane-anesthetized rats (Ito & Kato, 2002). Simons and coworkers (1992) coworkers have explicitly compared barrel cortex neuronal responses under urethane with those obtained in awake rats and observed the tonic component exclusively under urethane. The data presented in the next chapter of this dissertation were obtained in awake rats, and also contained not a single unit exhibiting a tonic response to whisker deflections (while it did indicate the presence of SA information in barrel cortex). Thus, at least on the basis of adaptation properties, there does not seem to be a segregation of RA and SA units in barrel cortex. However, this may be a premature conclusion.

Notably, the separability of SA and RA units need not be based on their adaptation profiles. Even though their names suggest that adaptation to a ramp-and-hold

deflection is the most reliable criterion on which to base a distinction, there is reason for criticism. SA units can, in fact, display an RA profile when their corresponding whisker is deflected at medium amplitudes only, or away from their preferred direction (Lichtenstein et al., 1990), leading to possible errors in classification. Moreover, the notion of adaptation might not really apply to RA neurons: it is not that they rapidly adapt to a ramp-and-hold deflection. Instead, as Fig. 2.5 shows, they are sensitive to velocity, not amplitude of deflection, and only the ramp phase of the whisker deflection contains non-zero velocities. Thus, they do not "adapt" during presentation of ramp-and-stimulus; instead, the specific stimulus they respond to, the ramp, is not present anymore. Taking this into consideration, subdividing the two classes of neurons might be more readily accomplished on the basis of velocity thresholds. As Figs. 2.4 and 2.6 show, SA units respond to velocities as low as 62 °/s with a considerable number of impulses, while reliable RA firing (> 1 impulse/stimulus) is not obtained at velocities lower than 1000 °/s (see Figs. 2.4 and 2.5); the majority of RA units encountered in the ganglion require much higher driving velocities. Therefore, a more straightforward subdivision of ganglion units might be achieved with two high-amplitude whisker deflections, one with a small ramp velocity, one with a very high ramp velocity, to classify SAs and RAs as low-velocity threshold and high-velocity threshold units.

In the same vein, if SAs and RAs projected separately to thalamus and cortex, the presence of a tonic response component to ramp-and-hold deflections were not required for a subdivision; instead, cortical units should fall into two major classes subdivided by their velocity and amplitude thresholds, with little overlap.

Tentative suggestions for channel functions

Irrespective of channel separability in thalamic or cortical whisker representations, the two channels might still be assigned different roles. The specific roles of the four human channels was identified using a combination of neurophysiological recordings, modeling studies, and further psychophysical experimentation (for a review, see Johnson et al., 2000).

Recently, the first behavioral observations with concomitant unit recordings in the trigeminal ganglion have been described (Bermejo et al., 2004; Leiser and Moxon, 2007). However, the rats were not engaged in any behavioral task and were just whisking while being head-fixed (Bermejo et al., 2004) or freely walking about (Leiser & Moxon, 2007). The latter authors showed that SA neurons fire both during whisker contact and whisking in air, while RA neurons almost exclusively discharge during contact.

Szwed et al. (2003, 2006) have recorded from the trigeminal ganglion in anesthetized rats. Through repetitive stimulation of the facial nerve, they generated rhythmic whisker motion which resembles natural whisking patterns. In an attempt to arrive at a more natural categorization of classes of ganglion units, they distin-

guished between "whisking cells" firing only during whisking in air, "touch cells" firing only during contact of a pole that intercepted the whisking trajectory, and "whisking/touch cells" that responded to both whisking in air and object contact. Comparing these response types with the classical subdivision of rapidly and slowly adapting cells, they found that both SA and RA cells fire during whisking in air, which stands in contrast to Leiser & Moxon (2007). One interesting observation they made concerns two subclasses of touch cells: so-called "pressure cells", which fired neither at the onset or offset of object contact but during the time the whisker pressed against the object, were exclusively slowly adapting, while "contact/detach cells" displaying the opposite behavior were exclusively rapidly adapting. Szwed et al. (2003) went on to place the pole at different horizontal positions with respect to the rat's head and attempted to reconstruct the pole's position from the firing patterns of individual cells. While both contact/detach and pressure cells conveyed some information about horizontal object position, the delay to the first spike after whisking onset in contact/detach cells provided by far the highest median information. In a modified experiment, pole position was varied in its radial distance from the rat's snout. Again, the capability of different unit classes to convey object position was assessed. Here, pressure cells provided more information than contact cells, though the effect was smaller than for horizontal object position.

Employing an information-theoretic approach, Jones et al. (2004ab) presented white-noise stimuli to individual vibrissae and measured SA and RA responses in the ganglion. Surprisingly, they found that RA and SA neurons were indistinguishable with respect to reconstructing the original stimulus waveform in terms of its amplitudes, velocity, and acceleration.

Though these observations are somewhat diverging, they might be brought together with more rigorous attempts to classify SA and RA units consistently across studies. As outlined in the previous section, SA and RA units are commonly classified according to the presence or absence of a tonic response component to ramp-and-hold stimuli. It was already suggested that this may lead to misclassifications, especially in terms of misclassifying SAs as RAs, because SA units do have RA-like profiles at lower amplitudes and when stimulated at an oblique angle to their preferred direction (Lichtenstein et al., 1990; Shoykhet et al., 2000). This is particularly problematic in Jones et al. (2004ab), in which a low-amplitude pulse was used to classify neurons; conceivably, many of their presumed RA units might turn out to be SA units when stimulated at a higher amplitude. In support of this, Jones et al. described neuron responses to white-noise stimuli lowpass-filtered at 25 Hz. At the amplitudes used by them, these stimuli do not contain velocities high enough to drive the class of RA units observed in our laboratory. Consequently, most or all of their presumed RA units may have been SA units, which would explain why Jones et al. found SAs and RAs indistinguishable with respect to stimulus reconstruction.

Taken together, one may arrive at tentative suggestions for functions of the chan-

nels and their respective neural correlates in the trigeminal ganglion. These suggestions are necessarily incomplete; striking capabilities of rats such as texture discrimination (Carvell & Simons, 1990) cannot be accommodated, because no data on the responses of the neuronal subclasses during such conditions has ever been recorded. However, on the basis of previous work discussed above and the study reported in this chapter, I advance the following three hypotheses:

Expansion of dynamic range. SA and RA units work in concert to cover a wide dynamic range in terms of velocities. SA spike counts in the peak response scale with velocity in the range from 62 °/s up to approximately 1000 °/s (compare Fig. 2.6c) but not beyond it, and RA spike counts start responding reliably (> 1 spike/stimulus) only at 1000 °/s and scale with velocities above it (Fig. 2.5; Shoykhet et al., 2000). Together, these two unit classes are capable of providing information about a wide velocity range.

The W1 channel mediates determination of radial object position. Szwed et al.'s (2006) paper shows that pressure cells (exclusively SA; aligned to the W1 channel) convey information about the radial position of a vertical pole and all neuronal codes examined ? delay to first spike after whisking onset, interspike interval, total spike count, and identity code (total number of pressure cells activated as a function of object radial distance). Conversely, contact cells (largely RA ? aligned to W2 channel) provide significantly less information about radial object position.

The W2 channel mediates determination of horizontal object position. As outlined above, Szwed et al.'s (2003) class of contact/detach cells consisted exclusively of RA units (aligned to the W2 channel) and quite precisely conveyed the horizontal position of a pole intercepting the whisking trajectory by spike timing relative to whisking onset, whereas pressure cells (exclusively SAs) did less so.

Preliminary conclusions

It is the major result of this chapter that perception in the rat whisker system displays similar principles of organization as the tactile sensing with finger tips in primates. As in primates, the whisker system relies on independent psychophysical channels defined by the association of specific sensitivity ranges (i.e. presumptive differing perceptual qualities) with respective response characteristics of the corresponding type of primary afferent. In humans, perception of different surfaces via the tactile modality is mediated through four such psychophysical channels (Bolanowski, et al., 1988). In order to fully exploit the similarities in organization of rodent whisker and primate finger tip system revealed here, the following issues have to be brought forward in future studies. First, the possible association of receptor classes to psychophysical channels has to be elucidated. At least six different types of nerve endings exist at the hair follicle (Ebara et al., 2002) and may represent the basis for such association. Second, specific behavioral functions have to be attributed to the psychophysical channels. In primates such functions (e.g. texture and form perception, skin motion,

hand formation, and distant vibration) have been successfully associated with certain psychophysical channels (Johnson et al., 2000). In contrast, it is unclear if and how suggested functions of the whisker system (e.g. texture discrimination, Carvell & Simons, 1990; egomotion, Szwed et al., 2006, etc.) are related to psychophysical channels. Third, the central representations giving rise to subjective experience have to be identified (de Lafuente & Romo, 2005). The realistic possibility that in rats relatively early stages in processing, e.g. barrel cortex activity with its exquisitely well studied microcircuits, are directly related to perception is an exciting prospect in terms of the quest how detailed neurophysiological processes relate to perception. The next chapter describes an attempt to find such neural correlates of subjective sensory experience in barrel cortex.

3 Signals representing detection and perception in the W1 channel in barrel cortex

3.1 Chapter introduction

Given the psychophysical description of the whisker system as consisting of at least two channels with different but overlapping kinematic response ranges put forward in the last chapter, it has become possible to study neural coding mechanisms in each channel in isolation. This chapter is devoted to the question as to which neural coding scheme ? lower envelope vs. any kind of response pooling ? underlies detectability of whisker deflections in the barrel cortex.

The W1 channel seems particularly interesting. In the previous chapter, I described that its peripheral correlates, the SA neurons of the trigeminal ganglion, are in fact more sensitive to slow whisker deflections than rat subjects. Accordingly, these neurons respond robustly to a low-velocity deflection which is perceptually subthreshold (62 °/s, Figs. 2.6ab). Successful alignment of psychometric thresholds with SA unit responses were only possible when counting spikes in a brief time interval of ˜ 4ms to 13 ms duration centered on the peak response in each fiber (which is a function of deflection velocity), thus ignoring the tonic response component. This implies that a large number of spikes in SA afferents may remain undetected.

In order to clarify these issues, I combined the psychophysical detection task with concomitant unit recordings from barrel cortex and tested the following hypotheses:

1) Cortical neurons' responses are consistent with my former result that detection performance in the W1 channel is based on a small number of spikes in the phasic peak response of ganglion units rather than the tonic response component. If this is correct, the tonic response component in SA trigeminal neurons should not be present in cortical neurons anymore, and detection performance of cortical neurons should be both optimal in and constrained to a spike integration window which is a function of deflection velocity and occurs at the same time after deflection onset as the ganglion spike peak for the respective stimulus velocity, offset by transmission delay from the periphery to cortex.

2) Even though SA ganglion units respond to velocities way smaller than rat observers, barrel cortex neurons should not. The finding that detection performance of rat observers is based on very few spikes during the phasic peak response of ganglion units rather than the tonic response component suggests that only the former should be reflected at higher integration levels of the nervous system such as the cortex. Individual cortical neurons may be equally or less sensitive compared to rat observers, but not more sensitive, because psychophysical performance is constrained by the spike information contained in the ganglion peak response.

This prediction is tantamount to saying that velocity thresholds in the W1 channel follow a lower envelope coding scheme at the cortical level. However, if barrel cortex neurons are considerably less sensitive than rat observers, it would favor a so-called response pooling/ideal observer model. In this case, the correlation between neuron responses had to be examined and pooling algorithms had to be constructed to see whether neurometric performance increases significantly by this combination to reach psychometric performance. Conversely, if a considerable fraction of barrel neurons were more sensitive than rat observers, it would support a simple "averaging" model and align with the findings of de Lafuente & Romo (2005) in monkey primary somatosensory cortex.

3) On a single neuron basis, the lower envelope principle predicts that the most sensitive neurons subserving detection should exhibit a significant trial-by-trial covariation with detection performance, because it is those neurons that, according to the lower envelope model, mediate the percept. Accordingly, if those most sensitive units fail to respond during a near-threshold trial, the observer has no percept and will therefore not report a detection.

3.2 Methods

Surgical procedures and the behavioral setup have been described thoroughly in chapter 2 as well as in (Stüttgen et al., 2006). Some procedures specific for the present study will be described below.

Chronic implantation of movable multi-electrode arrays and recordings

Three male Sprague-Dawley rats (Harlan Winkelmann, Borchen, Germany), aged 12-16 weeks) served as subjects. During head mount surgery, a trepanation over the barrel cortex was performed. The C1 barrel was located by mapping the cortex with a single intracerebral electrode. Unit and field potential responses to a brief manual whisker flick were monitored until a site maximally responsive to flicks of whisker C1 with lower activation by flicks of adjacent whiskers was found. Multi-electrode arrays (2x3 or 2x2, electrode distance ˜ 250 μm to 375 μm) were centered over the identified location of C1 and slowly inserted into the cortex at a speed of 1.25 μm/s until all electrodes had penetrated the dura (usually 300 μm to 800 μm). Then, the electrodes were slowly retracted to about 250 μm depth relative to the cortical surface. The cortex was covered with antibiotic ointment, and the electrode array was fixed to the skullcap with dental cement.

The movable electrode arrays contained laboratory-built pulled and ground glass-coated platinum tungsten electrodes (80 μm shank diameter, 23 μm diameter of the metal core, free tip length ˜ 8 μm, impedance: 2-6 M?; Thomas Recording, Giessen, Germany). Electrode depth could be adjusted by turning a small screw (one revolu-

tion equaling 250 μm). After each successful recording session, the screw was turned by a half revolution until the entire depth of the cerebral cortex was traversed. After that, the screw was turned up maximally and the procedure commenced again. Voltage traces picked up by the electrodes were band-pass filtered (200-10,000 Hz) and recorded at 20 kHz sampling rate using a multichannel extracellular amplifier (MultiChannelSystems, Reutlingen, Germany).

Spikes were detected using amplitude thresholds. 2 ms cutouts centered on the time bin in which the voltage trace first traversed the amplitude threshold were recorded and sorted offline using the laboratory-written software package SPS (Hermle et al., 2005). Artifacts were removed and neurons sorted to yield either single or multi unit spike trains. Criteria for single unit recording have been described in (Möck et al., 2006).

Spontaneous firing rates for each unit were computed from a 500 ms period preceding stimulus onset. Response latencies were calculated by measuring the time from stimulus onset (for the reference stimulus) to the time when the firing rate first surpassed a 95 % confidence limit which was computed based on the pre-stimulus firing rate (Abeles, 1982). Similarly, the width of the response peak in the PSTH (and, thus, the duration of the excitatory response) was calculated by measuring the time from the first traversion of the upper 95 % significance threshold to the time when the response decreased below the threshold.

Whisker stimulation

Whisker stimuli in this study were identical to those described in the previous chapter, but restricted to a subset of stimuli designed to preferentially activated the W1 channel. Here, the range of velocities covered was 5.4 mm/s to 130.9 mm/s, with all stimuli having a peak amplitude of 1100 ?m. These values correspond to 62 °/s to 1500 °/s for velocities and 12° for amplitude if applied 5 mm from the whisker base. In addition, a high-velocity rectangular pulse of ˜ 600 μm amplitude (7°) and ˜ 450 mm/s (5000 °/s) was used as a reference stimulus. Each stimulus was applied 10 to 25 times during the course of a behavioral session.

Data analysis and statistics

Psychometric functions. Psychophysical data are expressed either as response probability (no. of responses divided by no. of stimulus presentations) or as the signal detection theoretical index d' (Tanner, Jr. & Swets, 1954; Swets, 1961; Stanislaw & Todorov, 1999), which conveys the sensitivity of an observer stripped of response bias. Because of the low number of stimulus presentations in this study (10-25 per stimulus type), loglinear corrections were applied to control for response probabilities of 1 and 0 (Stanislaw & Todorov, 1999). For computation of d', response probability for signal trials ("signals" being one of five different peak velocities) was contrasted

with the response probability for noise trials ("noise" being catch trials) according to the formula , where ?–1 is the inverse of the phi function, which converts a probability to a z-score, HR is the response probability for signal trials ("hit rate"), and FAR is the response probability for noise trials ("false alarm rate"; for a collection of signal detection theoretical indices and formulas, see Stanislaw & Todorov, 1999).
Neurometric functions. To achieve comparability with psychometric functions, neurometric detection functions were computed using ROC (receiver operating characteristic) analysis (Tanner & Swets, 1954) as employed by Barlow & Levick (1969) and more thoroughly described by others (Vogels & Orban, 1990; Britten et al., 1992). Briefly, one looks at spike counts from signal trials of one session and compares this with spike counts from noise (catch) trials from the same session. Using a shifting criterion of n spikes, in which n shifts from the minimum spike count to the maximum spike count observed across both trial types, the fraction of both signal and noise trials featuring ? n spikes can be computed. This yields n measures of hits and false alarms for signal and noise trials, respectively. Typical ROC curves are shown in Figs. 3.4cd. The area under a given ROC curve gives an index of sensitivity (or choice probability; Britten et al., 1996), which expresses the amount of overlap between signal and noise (catch) spike count distributions. Sensitivity varies between 0 and 1, with 0.5 indicating complete overlap between the distributions and, thus, non-separability by any criterion value. Values of 0 and 1, on the other hand, indicate complete separation of the two distributions. Intuitively, the measure can be understood as the probability that an ideal observer counting spikes in both signal and noise trials could correctly distinguish between the two trial types. To compare psychometric and neurometric functions on the same scale, the area under the ROC curve was converted to d' using equation (11) in Stanislaw & Todorov (1999). To distinguish between two different concepts, I will refer to the area under the ROC curve as sensitivity when it was computed to contrast spike counts of signal vs. noise trials, and choice probability when it was computed to contrast spike counts to a single stimulus type, which were separated according to whether the rat responded to the stimulus or not. Note, however, that the mathematical procedures to compute these measures are identical.

Average spike counts for the analysis of choice probabilities were compared with t-tests for dependent samples; deviation of choice probabilities from 0.5 were assessed with one-sample t-tests. Corresponding power analyses were conducted with the freely available software GPOWER 3 (Faul et al., 2007). Effect size in the choice probability analysis was quantified using Hedge's g, given by , where mhit and mmiss are the mean average spike counts for hit and miss trials for the near-threshold velocity of 250 °/s, and sp is the square root of the pooled within-groups variance (Kline, 2004). All lines depict means and 95 % confidence intervals (CI) constructed from t distributions (Cumming & Finch, 2001) unless stated otherwise.

3.3 Results

The present data set consists of 100 multi unit and 24 single unit recordings, collected over 49 behavioral sessions from three rats. Each behavioral session comprised at least ten trials per stimulus, with a maximum of 25 (median = 18.5).

Psychophysical data

Fig. 3.1a plots psychophysical data obtained from one example animal. Each line depicts mean response probability as a function of peak deflection velocity. Thin gray lines depict mean response probabilities from each session conducted with this rat. The bold red line displays their mean with 95 % confidence intervals. Psychometric functions were very similar across sessions (Fig. 3.1a) and animals (Fig. 3.1b). The average psychophysical performance across animals plotted against the logarithm of deflection velocity is fit almost perfectly by a Weibull function (adjusted r2 = 0.99; Fig. 3.1b). Baseline (catch trial) performance averaged 0.13, reference stimulus performance around 0.93.

To check for possible effects of fatigue or motivation over the course of a single session, I computed rank-biserial correlations (Cureton, 1956) between the responses of the animal (coded 1 for hits, 0 for misses) and the trial numbers on which these two responses occurred. A substantial negative correlation between trial number and occurrence of a response would indicate a declining response rate. Fig. 3.1c displays the distribution of rank-biserial correlations between response vs. trial number for all sessions and all animals. As can be seen from Fig. 3.1c, correlations clustered close to 0 (possible range: -1 to +1), slightly extending more into the negative range, implying a weak trend towards a decline in response rate across each behavioral session. However, this trend was of very small magnitude (median: rrb = -0.15), confirming my impression that the animals were performing robustly over the course of a session.

Neurometric data

Fig. 3.2 plots peri-stimulus time histograms (PSTHs) of one representative multi-unit (Fig. 3.2a) and one single unit (Fig. 3.2b). With increasing deflection velocity, a clear peak spike response becomes visible shortly after stimulus onset. Qualitatively, one can see in the multi unit PSTH that the peak becomes progressively narrower, and that the response latency becomes shorter with increasing deflection velocity. Furthermore, an inhibitory response followed the excitatory peak was observed (Fig. 3.2ab, arrows). This inhibitory response component was visible in nearly all PSTHs and has previously been described by others (Carvell & Simons, 1988; Webber & Stanley, 2004; Moore & Nelson, 1998; Zhu & Connors, 1999).

The presence of a tonic response component was checked by examining the width of the response peak in each unit's PSTH to the reference stimulus. The response

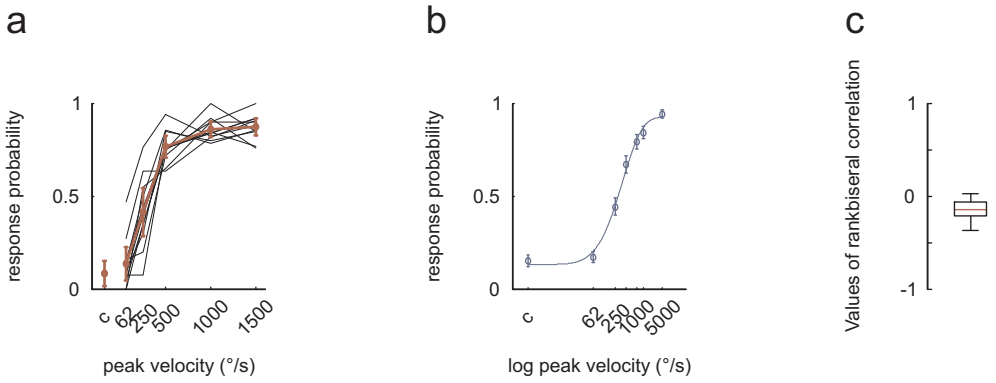

Figure 3.1: Psychometric data. a) Psychometric detection curves of one example animal as functions of peak deflection velocity (in °/s). Thin lines represent individual sessions, bold red line represents mean performance, error bars encompass 95 % CIs. b) Psychometric detection curves as functions of the logarithm of peak deflection velocity, for all three animals. Blue line represents Weibull fit of mean psychometric performance across all animals, circles depict individual data points with 95 % CIs. c) Boxplot of rank-biserial correlations between lick responses and trial numbers for all sessions of all animals. Red horizontal line depicts the median, box ranges from the 1st to the 3rd quartile. Whiskers encompass whole data range.

widths (see methods) ranged from 1 ms to 43 ms (median: 2 ms), with 95 % of data points being smaller than 21 ms. Therefore, tonic responses to sustained deflections, as found in SA ganglion cells (see Fig. 2.4) for several hundred milliseconds, were completely absent.

112 of the 124 units comprising the entire data set showed a significant elevation of firing rate within the first 100 ms in response to the fastest deflection of whisker C1. Calculated response latencies to the high-velocity stimulus ranged from 2 ms to 28 ms with a median of 7 ms, 1st and 3rd quartiles at 5 ms and 8 ms, respectively, and 95 % of recordings below 11 ms (Fig. 3.2c). These values are very close to response latencies observed by other investigators in the barrel cortex of awake rats (Fanselow & Nicolelis, 1999) or even shorter (Simons et al., 1992). This confirms that the bulk of the electrodes were indeed located in C1's receptive field, probably in or close by C1's principal barrel and, thus, are involved in processing signals from the C1 whisker.

Mean spontaneous activity was 22.96 Hz and 7.02 Hz for multi and single units, respectively (Fig. 3.2d).

Integration window analysis

Based on previous results in the trigeminal ganglion (Stüttgen et al., 2006), it was hypothesized that the best time point after deflection onset to look for spike responses to faint whisker deflections was determined by the peak spike response in trigeminal ganglion units (see chapter 2). Reanalyzing ten ganglion units from that data set revealed a considerable effect of peak deflection velocity on peak latency (Fig. 3.3a)

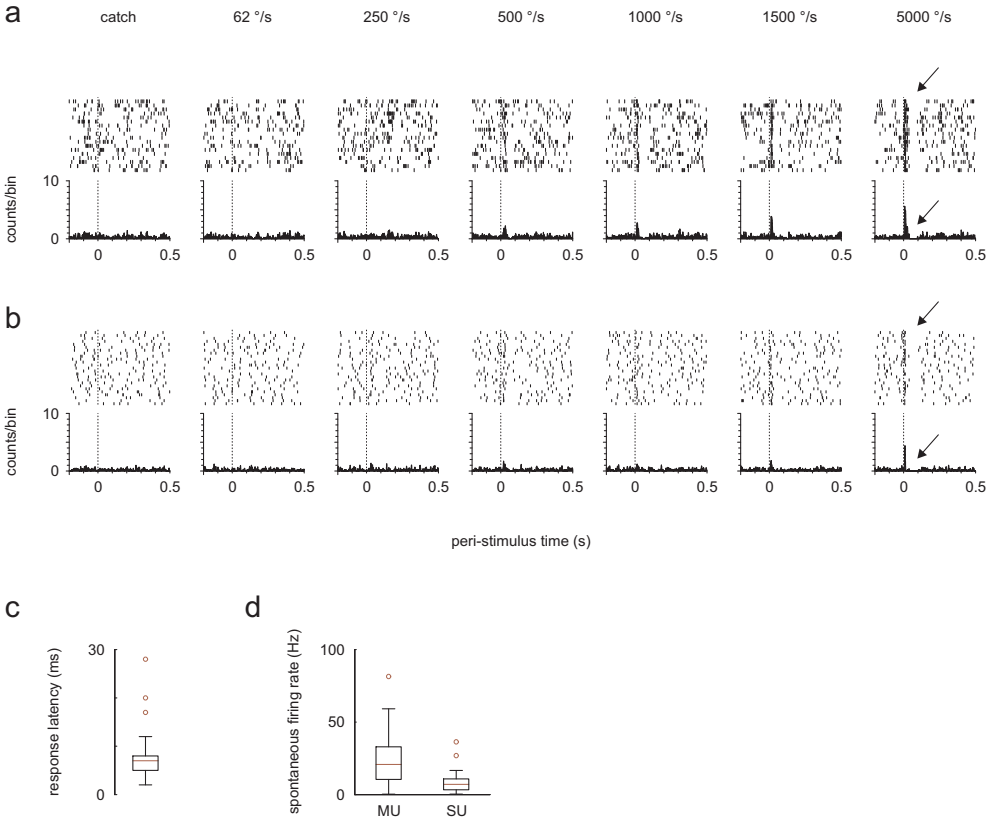

Figure 3.2: Example raster plots and PSTHs for a) one multi unit and b) one single unit. Stimuli delivered were catch trials (no actual stimulus), five different ramp-and-hold deflections with ramp peak velocities varying from 62 °/s to 1500 °/s), and a high-velocity (5000 °/s) square-wave pulse used to monitor performance and to check whether the unit of interest could be driven by C1 whisker deflections. Bin width = 1 ms. c) Boxplot of response latencies to the fastest stimulus. Box borders extend from the 1st to the 3rd quartile, whiskers encompass whole data range or, alternatively, 1.5 times the interquartile range; in the latter case, the position of data points outside 1.5 times the interquartile range (outliers) are depicted by red circles. d) Boxplots of spontaneous firing rates plotted separately for multi units (MU) and single units (SU). Conventions as in c).

as well as on latency variability, as indicated by size of the boxes spanning the 1st and 3rd quartiles.

While it seemed reasonable to center the integration windows in which to count spikes on the time of the median peak latency of ganglion neurons for the respective deflection velocity plus the median transmission latency from ganglion to cortex, the variability of peak latencies forbids the choice of relatively small integration windows. My previous results (see chapter 2, Fig. 2.6) indicated that window durations between approximately 4 and 13 ms yielded the best match of neurometric and psychometric curves (with r2 $>$ 0.95). However, the interquartile range of peak centers in the ganglion spans between 180 ms for the slowest (62 °/s) and ˜ 5 ms for the fastest stimulus (1500 °/s), with values of 41 ms, 9 ms, and 6 ms for 250 °/s, 500 °/s, and 1000 °/s, respectively.

Therefore, several combinations of window durations and window positions were examined to find a combination yielding optimal neuronal sensitivities (see section 3.2 for computation of sensitivity). The analysis encompassed a wide range of window durations (5, 10, 15, 25, 35, 50, 75, 100, 150, and 200 ms) and window positions (centered at 0, 5, 10, 15, 25, 35, 50, 75, 100, 125, 150, 175, 200, 225, 250, and 300 ms relative to stimulus onset). Sensitivity was computed for every possible combination of window durations and window positions for all stimuli at each velocity for all barrel cortex units. Mean sensitivity as a joint function of window duration and window position for all five stimuli is shown in Fig. 3.3b, with hotter colors representing higher sensitivity. Blue squares mark the window position predicted from the ganglion peaks, for a window duration of 25 ms. It can be seen that, with the exception of the slowest deflection velocity, predicted and optimal window positions coincide nicely. While the range of optimal window positions was relatively narrow, a relatively broad range of integration window durations yielded good results, with optimal values ranging from 15 to 35 ms duration. Therefore, I decided to base all consecutive analyses on an intermediate window duration of 25 ms, combined with window positions obtained from ganglion data. The deviation of predicted and optimal window positions for the slowest deflection is unproblematic, because this stimulus was neither detectable by the rat observers, nor by the units. Thus, no "hot spot" of sensitivity could be expected, which is supported by the uniform appearance of the corresponding panel in Fig. 3.3b.

Fig. 3.3b also shows that, right after the hot colors signifying maximum sensitivity values, a parallel stripe at cooler colors than the uniform background is visible, especially at higher velocities. This is due to inhibitory response following the fast excitation visible in many units (see Figs. 3.2ab). Since the strength of both excitatory and the inhibitory response components is a function of peak velocity, it is unclear which one of these components carries more information in terms of sensitivity. The data from Fig. 3.3b are replotted in Fig. 3.3c such that colors now represent sensitivity as an absolute deviation from the chance value of 0.5 (absolute sensitivity = |

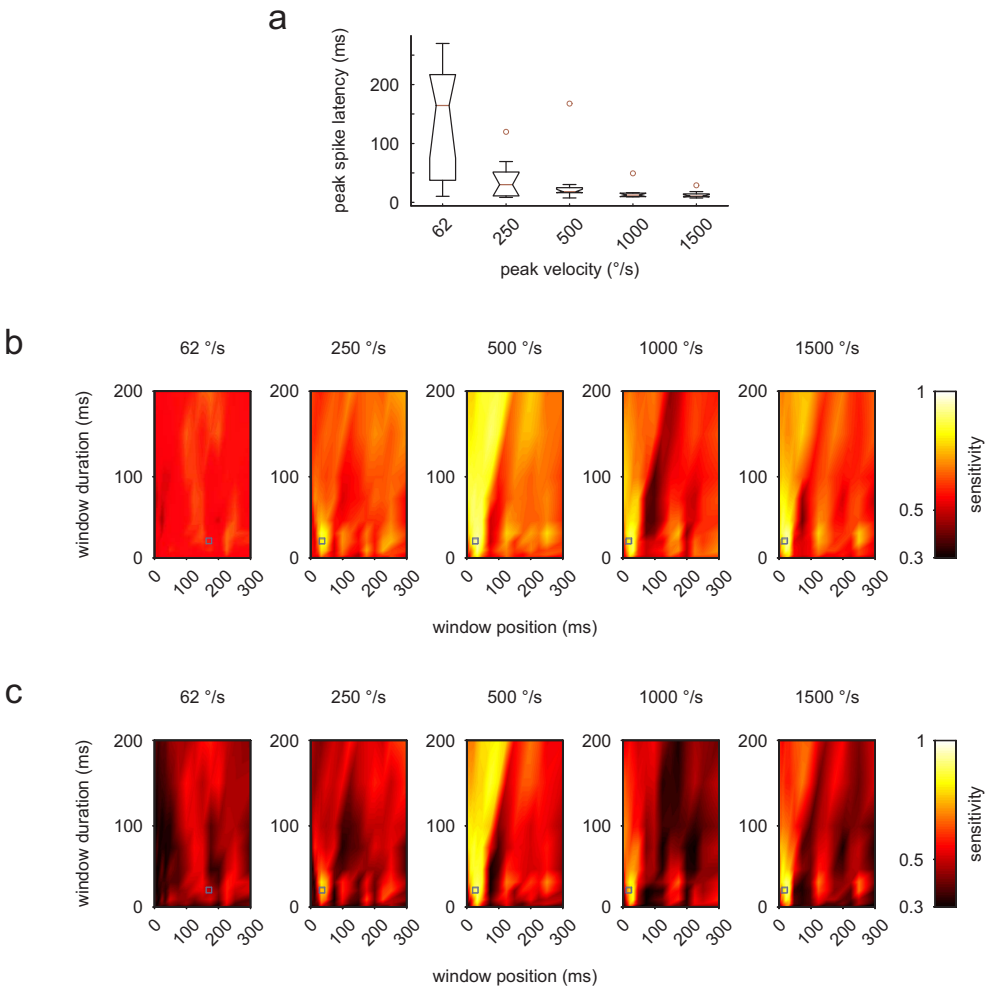

Figure 3.3: Integration windows analysis. a) Boxplots of peak spike latencies for ten slowly adapting ganglion units as a function of peak velocity. Conventions as in Fig. 3.2, notches represent 95 % CIs for the median. b) Results of window analysis for all animals together. Each panel depicts sensitivity of spike counts to one of five different peak velocities when contrasted with catch trials, for 10 different window durations and 16 different window positions. Sensitivity is pseudocolor-coded, with values of 0.5 representing equal spike count distributions in stimulus and catch trials, while values > 0.5 represent higher spike counts during signal trials, and values < 0.5 represent lower spike counts during signal trials. Blue squares depict hotspots predicted from median ganglion latencies plus 7 ms delay to cortex, with 25 ms window duration. c) Same data as in b), but normalized to show hotspots of sensitivity irrespective of excitatory or inhibitory response (see methods). Here, sensitivity is measured as the absolute deviation from chance (0.5; see text).The excitatory response confers a significantly higher sensitivity than the inhibitory response.

sensitivity ? 0.5 |). Fig. 3.3c shows that, while the inhibitory response component carried obvious sensitivity, it was substantially lower than that of the excitatory response component. Taken together, this supports the notion that basing the following neurometric analyses on spike counts obtained in 25 ms wide windows centered at the peak of the ganglion response (offset by 7 ms response delay in the cortex) did not underestimate the sensitivity of the neurons, but instead represents the maximum sensitivity these neurons are capable of signaling.

Sensitivity analysis

Fig. 3.4 describes the ROC analysis of a representative multi unit (left panels) and one single unit (right panels) from the same animal. The distributions of spike counts for windows of 25 ms duration, centered on the timing of the peak ganglion response plus 7 ms delay to the cortex are shown in Fig. 3.4a.

Fig. 3.4b shows ROC curves computed from the distributions in Fig. 3.4a. Sensitivity (bending of the curve towards the upper left of the graph; area under the curve) of signal and catch trials increases with peak deflection velocity for both the multi unit and the single unit. A quantitative index of sensitivity is the area under the ROC curves. As described in methods, this value may extend from 0 to 1, with 0.5 implying non-separability of signal and noise distributions. Integrating the five ROC curves in each panel of Fig. 3.4b yields five data points which are plotted as a function of velocity in Fig. 3.4c. Dotted horizontal lines represent zero sensitivity for comparison. For both the multi unit and the single unit, sensitivity tended to increase with increasing velocity, and saturated at around 0.85. In addition to the straightforward implication that velocity drives these neurons, it indicates that an observer relying on spike counts within the specified integration window could tell the presence of a stimulus in a certain percentage of cases, given by the integrated area under the ROC curve (sensitivity).

Note that the maximum spike count within the chosen integration window was only four for the multi unit and two for the single unit. Nonetheless, a considerable fraction of stimuli can be detected with two spikes only, as Figs. 3.4bc show.

Comparison of psychometric and neurometric data

Signal detection theory offers a convenient framework for the comparison of psychometric and neurometric data ? the index d'. Both the dependent measure for psychometric data, response probability on signal and catch trials, and the dependent measure for neurometric data, here called sensitivity, can be easily converted to d' (see methods). Plotting the mean psychophysical performance of all animals with 95 % confidence intervals in units of d' together with neurometric curves on the same scale shows that the psychometric curves, with few exceptions, form the upper boundary for the neurometric curves. This holds for both multi units and single units

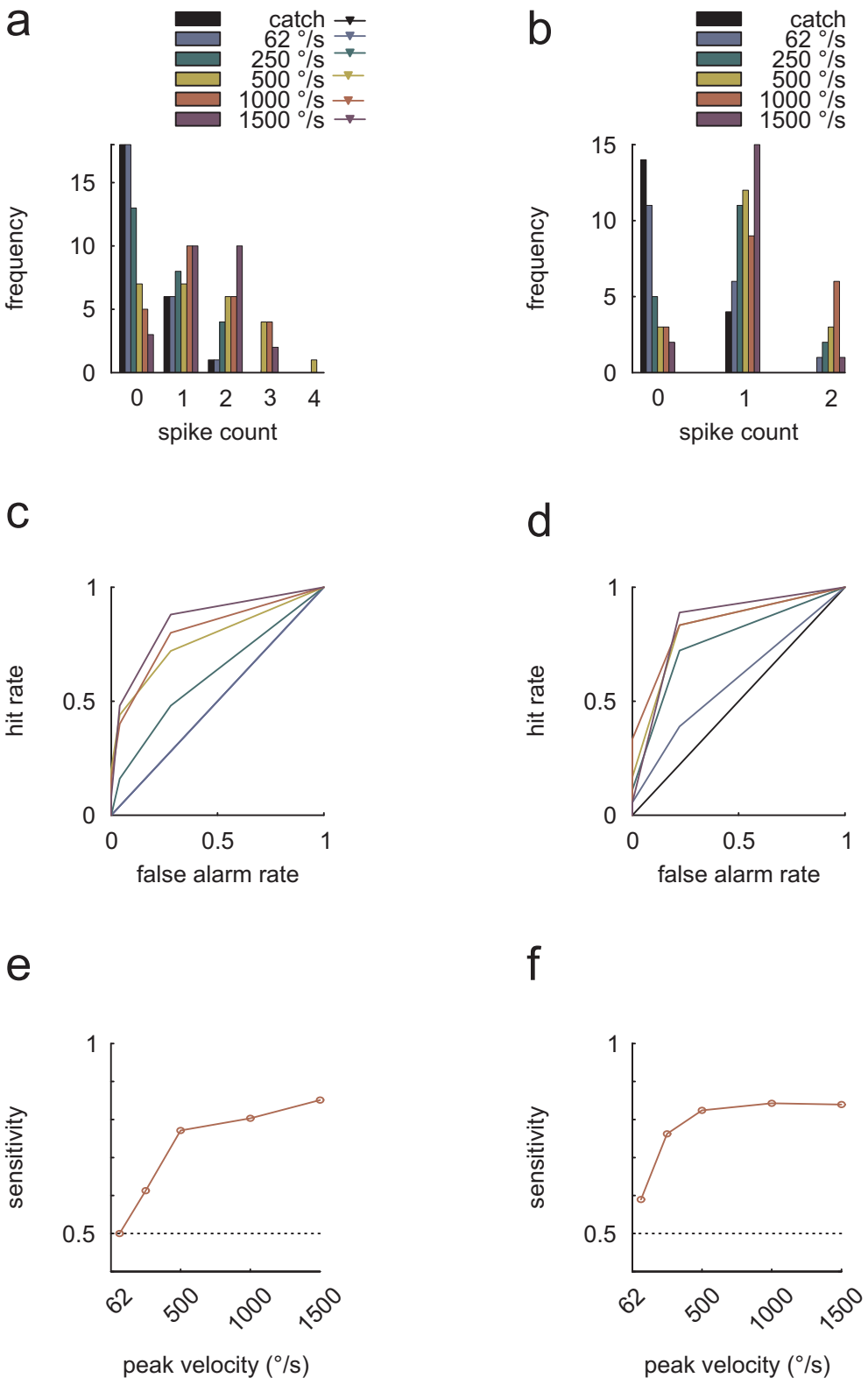

Figure 3.4: ab: Example distributions of spike counts within 25 ms windows for five stimuli and catch trials. Left panels: multi unit, right panel: single unit. cd: Neurometric ROC curves for spike responses to five different deflection velocities contrasted with catch trials. See methods for construction of neurometric ROC curves. Dark blue diagonal line: chance performance. ef: Neurometric functions derived from ROC curves. Dotted line, chance performance.

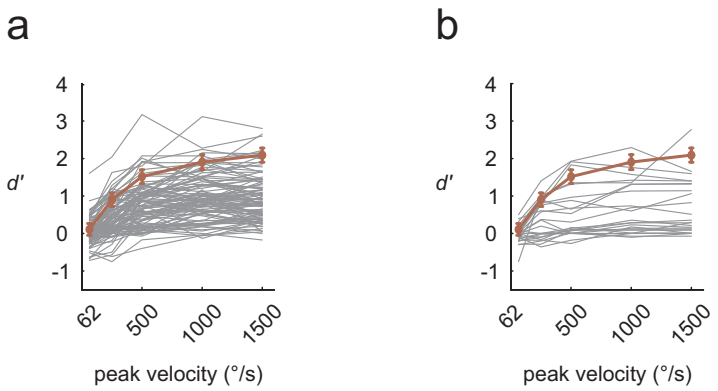

Figure 3.5: Comparison of psychometric and neurometric detection curves for multi units (a) and single units (b). Bold red lines: mean psychophysical performance (expressed as d') +/- 95 % confidence intervals. Thin gray lines: neurometric functions for individual multi units or single units computed from ROC analyses.

(Figs. 3.5ab, respectively). Note that this is not the consequence of recording at the wrong sites; 112 of 124 units contained in the analysis were significantly driven by suprathreshold whisker deflections, and the correct location of the electrodes within the receptive field of whisker C1 was ensured by mapping during implantation and later confirmed by electrophysiological criteria (short firing latencies and the presence of a significant response to the fastest deflection).

Choice probability

The next analysis was conducted to examine whether the response of the animal to a near-threshold whisker deflection (250 °/s), presumably reflecting the presence or absence of a percept, could be predicted from spike counts in the stimulus' optimal integration window. To do this, trials from individual sessions were separated according to the presence or absence of a lick response (hit and miss trials, respectively), and their respective spike counts were compared.

Figs. 3.6ab plot the distributions of spike counts for hit (red) and miss (blue) trials for multi and single units, respectively. Average spike counts were low, ranging from 0 to 4 spikes, and obviously non-normally distributed. Figs. 3.6cd present these data as boxplots, separated for hits and misses. The immense overlap of box notches (representing 95 % confidence intervals) suggests the absence of any noteworthy difference between average spike counts. Furthermore, the 95 % confidence interval for the difference between average spike counts spans -0.18 to 0.003 (multi units; range of average spike counts 0 to 4) and -0.16 to 0.16 (single units; range 0 to < 2). The failure to find a significant effect for multi (t-test for dependent samples: t = -1.9, df = 99, p = 0.06) and single units (t-test for dependent samples: t = -0.02, df = 23, p = 0.99) is not due to insufficient statistical power; with a sample size of n = 100 pairs (MU) and the observed correlation between hits and misses for identical units

of r = 0.82, a t-test for dependent samples has a power of > 0.99 for detecting a medium-sized effect (Hedge's g of 0.5) and still a power of 0.7 for detecting an effect size half as large. This considerably exceeds the range of statistical power usually found in experimental studies. While the corresponding power values for the single units is somewhat smaller (0.65 for g = 0.5), the very small observed effect size (g < 0.003) also argues against the existence of a substantial difference.

Figs. 3.6ef plot choice probabilities for multi and single unit data. Individual data points are relatively symmetrically distributed around the medians of 0.52 (multi units; range: 0.32 to 1, 1st and 3rd quartiles are 0.43 and 0.59) and 0.5 (single units; range: 0.26 to 0.73, 1st and 3rd quartiles are 0.46 and 0.56).

The analysis above does not exclude the possibility that a subset of neurons, e.g. the most sensitive ones, have either very large or very small choice probabilities, depending on the direction of the effect. Thus, as a last check, I investigated whether a given unit's sensitivity to the near-threshold stimulus was correlated with its choice probability derived from the perceptual report of the animal. The scatterplots in Figs. 3.6gh show that no apparent relationship between the two variables existed. Moreover, the correlations between the two measures were small (MU: r = 0.07; SU: r = 0.03) with their 95 % confidence boundary extending both into the positive and negative range (SU: 95 % CI [-0.38 0.42]; MU: 95 % CI [-0.13 0.26]). It can be concluded that the response of the animals to a near-threshold stimulus cannot be predicted from unit spike counts in barrel cortex. Note that this is an explicit demonstration of the absence or near-absence of a perceptual effect on primary sensory cortex neurons' firing behavior. The absence of an effect can not be demonstrated by showing that the p-value of a null-hypothesis significance test does not reach the common 0.05 level of statistical significance, because of the lack of regard for statistical power (Cohen, 1994). Therefore, a power analysis was conducted to show that, if an effect exists, it must be of very small magnitude, likely smaller than that which I found.

3.4 Chapter discussion

Employing a psychophysical detection task, I found that the perceptual thresholds of the animals were reached but very rarely exceeded by single units or multi units in barrel cortex. This implies that the perception of faint tactile stimuli must be based on a relatively small subset of neurons which are most sensitive to near-threshold whisker deflections. The time points of highest neuronal sensitivity predicted on the basis of ganglion SA units' peak spike response were very close to those determined by an empirical analysis of cortical units. This strengthens the hypothesis put forward in chapter 2 and in Stüttgen et al. (2006) that it is a small number of spikes occurring in rapid succession in SA trigeminal neurons which determine the occurrence of a percept rather than the total number of spikes emitted. Furthermore, the excitatory part of the neuronal response carries considerably more information than the inhibitory component. However, the search for a trial-by-trial covariation of neuronal and psy-

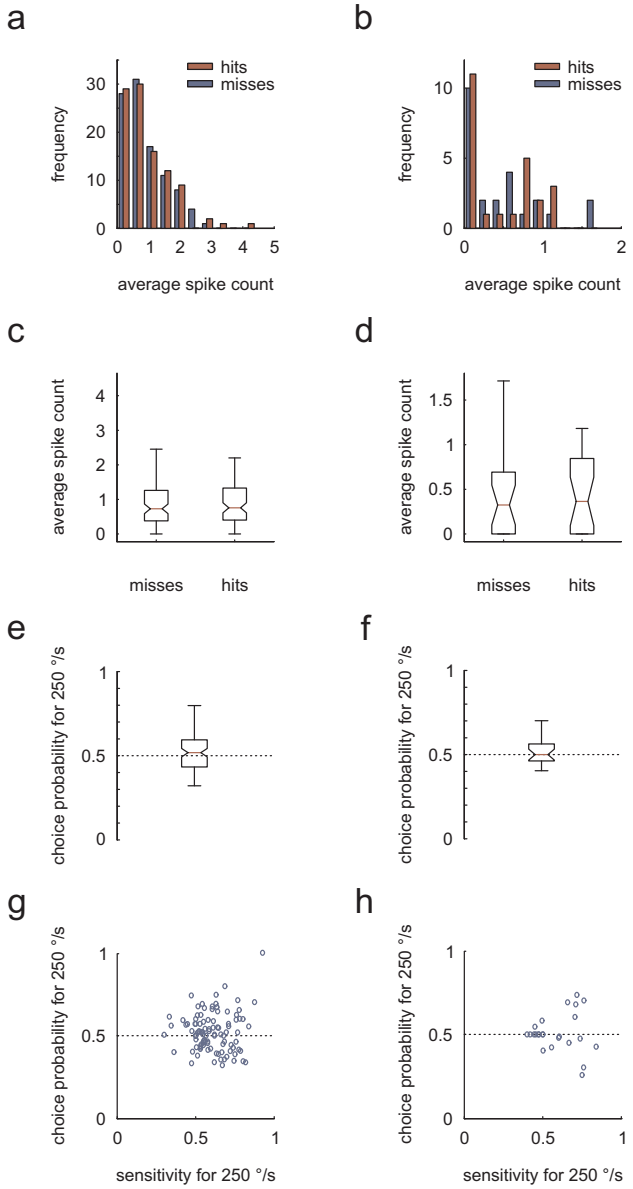

Figure 3.6: Choice probability analysis for multi units (left panels) and single units (right panels). ab: Frequency histograms of average spike counts in hit (red) and miss (blue) trials. cd: Boxplots of the data contained in ab. Notches represent 95 % confidence intervals. ef: Boxplots for choice probabilities; dotted line represents chance. gh: Scatterplots showing sensitivity of a given unit for the near-threshold stimulus vs. the unit's choice probability. Dotted line represents chance choice probability.

chophysical responses to a near-threshold stimulus was unsuccessful; consideration of statistical power revealed that this was not due to insufficient sample size, especially for multi unit recordings.

Below I discuss the following aspects: a) whether the choice of a go-task for the detection paradigm might yield an over- or underestimation of psychophysical thresholds, and b) whether the primary reliance on multi vs. single units has a notable effect on the conclusions. The last aspect to be addressed concerns the tenability of the hypotheses stated in the introductory section of this chapter (c).

Impact of type of detection task on estimation of psychophysical thresholds

It has long been acknowledged that different psychophysical methods and procedures may yield different threshold estimates for identical stimulus sets (see e.g. Blackwell, 1952; Jäkel & Wichmann, 2006; Sakitt, 1972; Blough & Blough, 1977). For human subjects, Sakitt (1972) showed that conventional yes-no procedures yield threshold estimates substantially higher than those obtained with forced-choice procedures.

For our present purposes, the question is whether the go-task implemented here yielded artificially high or low psychophysical thresholds that could counter the conclusion that very few neurons in barrel cortex match or even outperform rat observers. It is unlikely that the estimates of psychophysical detection thresholds reported in chapters 2 and 3 are artificially high. Firstly, the animals worked steadily for the entirety of the whole sessions, as is evidenced by both the very high response probabilities to suprathreshold reference stimulus (mean = 0.94) and the low values of the rank-biserial correlations between trial number and response occurrence (median = -0.15), indicating that response probability remained very constant across the whole session. Secondly, the rats were only mildly discouraged from emitting false alarms. I allowed for a low but non-zero response probability on catch trials (typically around 13 %), whereas in yes-no procedures human subjects are more strongly discouraged to emit any false alarms, thereby yielding elevated threshold estimates (Sakitt, 1972).

Similarly, it seems unlikely that the reported estimates of psychophysical detection thresholds are artificially low. Firstly, intertrial intervals varied randomly around 5 s by 25 % (1.25 s) in both directions; in combination with a very short response window of 600 ms, this considerably decreased the likelihood of the animal obtaining rewards just by random licking. Secondly, animals were mildly discouraged from emitting too many false alarms by shifting stimulus onset by 1 s in case of random licking during a 1 s period prior to scheduled stimulus onset. Consequently, this procedure yielded a low to moderate number of false alarms (on the order of ˜ 13 %). Low but non-zero false alarm rates likely represent the optimum between the response criterion being either too conservative (yielding elevated threshold estimates) and too liberal (yielding reduced threshold estimates). In addition, it was already shown that threshold estimates from the detection task can be well reconciled with the responses of trigeminal ganglion units (chapter 2; Stüttgen et al., 2006), further supporting the

claim that the threshold estimates are precise. Finally, and most importantly, signal detection theory was applied to yield d' values instead of response probabilities for the comparison of psychometric and neurometric data. The metric d' has been shown by several investigators to be robust to both changes in methods and procedures and to changes in response criterion (conservative or liberal response bias; for an overview, see Tanner & Swets, 1954; Swets, 1961).

Single units vs. multi units

Previous investigators of similar questions have almost exclusively focused on single unit recordings as opposed to recording multi units (e.g. Mountcastle et al., 1990; Romo & Salinas, 2003; de Lafuente & Romo, 2005; Tolhurst et al., 1983; Britten et al., 1992; Britten et al., 1996). A predominant reliance on multi unit recordings might qualify the interpretations derived from these findings. Thus, if one of the neurons comprising a multi unit was more sensitive than the other neurons in the unit, its contribution to detectability was potentially obscured by the variability of the less sensitive units. Conversely, if the most sensitive neurons were clustered, a multi unit would be more reliable than each of its comprising neurons because noise variability tended to cancel out, while the (correlated) signal activity remained relatively stable. These qualifications hold for both the sensitivity and the choice probability analysis.

To control for this possibility, all of the affected analyses were conducted and presented separately for the two types of recordings, and the results were compared. None of the instances displayed any notable differences. Thus, it may be tentatively concluded that primary reliance on multi unit recordings carries no substantive problems for my interpretations. Moreover, the relatively small difference in spontaneous firing rates between multi units and single units (23 Hz vs. 7 Hz, respectively; cf. Fig. 3.2d) can be taken to imply that multi units comprised, on average, only about three neurons.

Indeed, the fact that some multi units reached the performance level of the observers may suggest that the most sensitive neurons are clustered in barrel cortex. Since I explicitly targeted the W1 channel and expected no contribution of the W2 channel, the most sensitive units in the sample may receive predominantly SA input. As discussed in the previous chapter, mapping of receptor types has been frequently demonstrated in monkey somatosensory cortex (e.g. Sur et al., 1984). Mapping of barrel cortex according to submodalities has yet to be done.

Tenability of hypotheses stated in introductory section

In the introductory section, I stated three hypotheses concerning the behavior of cortical neurons. The first hypothesis concerned whether previous results of psychophysical detection being based on a small number of spikes during the phasic response component of SA ganglion neurons rather than a large number of spikes during the

tonic response component was reflected in barrel neurons' firing pattern. Consistent with predictions, no tonic response component was observed in cortical neurons. Furthermore, maximal neurometric sensitivity was achieved if spikes were counted during integration windows centered close to those predicted by peak responses in SA ganglion units. These findings indicate that, indeed, the tonic response component of SA cells is filtered out completely by the time the SA signal reaches the cortex. To my knowledge, a tonic response component to ramp-and-hold deflections in cortex was only found when recordings were performed under urethane anesthesia (Simons et al., 1992; Ito & Kato, 2002), and the total absence of tonic responses in the present dataset support the conclusion that this response component is not present in the awake brain.

This is indicative of a high-pass filtering process between cortex and the sensory periphery in which spikes occurring at low firing rates are filtered out. The question why such a considerable number of spikes carrying potentially important information is discarded can, at present, not be conclusively answered. However, an analysis of the ganglion data (Stüttgen et al., 2006; chapter 2) showed that amplitude coding for ramp-and-hold stimuli is almost as good with very short integration windows as with considerably longer windows. Therefore, discarding spikes fired during the tonic component is efficient insofar as the relevant portion of the information is already in at the time the integration window closes. Moreover, it could be that both SA and RA neurons are used to signal transients in the environment (Jones et al., 2004ab). Since rats whisk most of the time during exploration (Welker, 1964), steady deflections ($>$ 100 ms) may occur rarely.

The second hypothesis was that detectability of a whisker deflection is limited by the most sensitive neurons available. This hypothesis is a direct consequence of the former result that, even though individual ganglion units signal very small velocities to the brain (cf. Fig. 2.6a), the rat obviously does not make use of it, as the non-detectability of the slowest stimulus in the psychometric detection curve indicated. To a large degree, this prediction was also confirmed. However, I observed units that indeed displayed a somewhat higher sensitivity than the rat observers. Nonetheless, the number of units exceeding the 95 % confidence intervals of the psychometric curve was very small. In those few cases, the absolute superiority of the neurons was only 0.3 (expressed as a difference in d') with the exception of one multi unit. Since the number of repetitions for each stimulus type never exceeded 25, some variability regarding estimation of "true" sensitivity of the unit is to be expected. More importantly, none of the recorded units even got close to the theoretical performance set by the SA ganglion units ? which is perfect detectability of even the lowest velocity employed in this study.

By and large, the data so far can be taken to support the lower envelope coding scheme in barrel cortex. However, at least in its stringent form, the lower envelope principle is not sufficient to account for the present data on two grounds: firstly, the

mere fact that there indeed were units matching the animals performance renders it unlikely that these units were the only ones that provided the relevant signals, because the sample size of 100 multi and 24 single units is hardly large enough to ensure detection of this one unit, even less so since there were such units in each individual animal subject. Secondly, the lower envelope principle (again, in its stringent form) implies that, even if one identifies this very neuron, its failure to fire on a given trial should lead the observer to lack a percept (prediction # 3). This prediction was not met. I observed only a very weak association between choice probability and sensitivity across all units. This indicates that the percept must have been supported by more than one neuron in barrel cortex.

In a slightly modified form (see Parker & Newsome, 1998), the lower envelope principle can be taken to imply that, while a single, very sensitive neuron is sufficient for a sensation (one of Barlow's (1972) "pontifical cells"), it need not be the same neuron on every trial. Accordingly, a number of sensitive neurons might share the job; thus, one of those neurons firing on a trial may be sufficient, but only if all of those neurons fail the percept is absent. A "relaxed" version of the lower envelope principle might allow for a small number of neurons required for a percept, with the qualification that there is no good data to estimate what is meant by "small".

In any case, a relaxed lower envelope account seems, at present, more appropriate than any of the variants of pooling models. Firstly, an "averaging account" of sensitivity such as that showed by de Lafuente & Romo (2005), in which the average neuronal sensitivity of units equals that of the observer, is not supported by the barrel cortex data (see Fig. 3.5). Secondly, an "ideal-observer response pooling account" such as that put forward by Johnson et al. (1973) need not be invoked to enhance overall neuronal sensitivities to match observer performance. Instead, the best barrel cortex neurons already do this. Thirdly, a response pooling model in which the contributions of the most sensitive elements are obscured by less sensitive ones (Britten et al., 1992; Shadlen et al., 1996) is again at odds with the data, since no neurons were found that considerably exceeded psychophysical performance. Thus, none of these three variants of response pooling can explain the data better than a lower envelope account.

4 Conclusion and outlook

How can we disentangle the neuronal circuitry of perception in the whisker system? Clearly, much can be learned from paradigms already applied in research on the primate tactile system. For example, individual channels may be temporarily inactivated or masked by adequate tactile stimulation (Bolanowski et al., 1988), or isolated by restricting stimulus parameters (Verrillo, 1963, 1965; Bolanowski et al., 1988; Stüttgen et al., 2006). On a neurophysiological level, different surfaces may be presented to the whiskers while the activity of first-order afferents is recorded (Johnson & Lamb, 1981; Benison et al., 2006), e.g. to see which of the neuronal subgroups conveys more information about texture (Jones et al., 2006; Hipp et al., 2006). Furthermore, to broaden the description of the whisker system on a psychophysical level, it seems demanded to introduce novel behavioral paradigms which allow for the assessment of discrimination thresholds (LaMotte & Mountcastle, 1975; Harvey et al., 2001).

It is exciting that such questions may be addressed in the rat whisker system. To date, most of our knowledge on the physiology of perception is derived from experiments on trained monkey observers. However, the whisker system possess some unique advantages. One such advantage is the presence of a lissencephalic brain: electrode recordings in rat barrel cortex can be precisely located to individual cortical layers, either by reading them off a micromanipulator during an acute experiment, or by placing small lesions directly after recording for verification with post-mortem histology. By comparison, monkeys are usually used in several consecutive experiments, and the precision of histology is lower. Moreover, their gyrated brains make a clear assignment of cortical layer difficult in chronic experiments (Powell & Mountcastle, 1959). In a similar vein, much of rat cerebral cortex, and especially the barrel subfield, is suitable for optical imaging and thus lends itself ideally to the assessment of function on the subcellular and molecular level e.g. by applying two photon microscopy (Kerr et al., 2005). Furthermore, rodent preparations are highly suitable for local genetic manipulation e.g. using viral vectors.

Another advantage of the whisker system stems from its role in active perception. As described in the introduction, whiskers are swept rhythmically across objects during exploration (Welker, 1964), and rats adjust their whisking parameters to object properties (Carvell & Simons, 1995). This makes the system an excellent model system for active perception, as it must solve principal computational problems of integrating movement and tactile signals. At the same time, it entails the advantage that explorative whisker movements can be described by simple models comprising essentially two degrees of freedom. This is in contrast to the complex finger movements in primates. Recently, Gao et al. (2003) elegantly described how whisking parameters can be brought under experimental control and top-down modulation of tactile processing in barrel cortex, presumably originating in primary motor cortex, has been shown (Hentschke et al., 2006).

In summary, the rodent whisker system is an exquisitely well described sensory system. The advantages over primate sensory systems lie in the detailed knowledge of microcircuits and its excellent accessibility and flexibility. Furthermore, mechanisms of plasticity on the structural (maps) and cellular (spines/dendrites) and synaptic levels (synaptic gain) have been described in this system. The advent of measurements of sensory and perceptual signals in combination with (multi) neuron recordings in the head-fixed animal as accomplished in this work is an important advance to help the system to come of age, and assist in the challenge for finally bridging the levels from the percept down to the molecule.

5 References

1. Abeles M (1982) Quantification, smoothing, and confidence limits for single-units' histograms. J Neurosci Methods 5: 317-325.

2. Ahissar E, Sonic R, Haidarliu S (2000) Transformation from temporal to rate coding in a somatosensory thalamocortical pathway. Nature 406: 302-306.

3. Andermann ML, Ritt J, Neimark MA, Moore CI (2004) Neural correlates of vibrissa resonance: Band-pass and somatotopic representation of high-frequency stimuli. Neuron 42: 451-463.

4. Arabzadeh E, Petersen RS, Diamond ME (2003) Encoding of whisker vibration by rat barrel cortex neurons: implications for texture discrimination. J Neurosci 23: 9146-9154.

5. Barlow HB (1972) Single units and sensation: a neuron doctrine for perceptual psychology? Perception 1: 371-394.

6. Barlow HB, Levick WR (1969) Changes in the maintained discharge with adaptation level in the cat retina. J Physiol 202: 699-718.

7. Barth DS (2003) Submillisecond synchronization of fast electrical oscillations in neocortex. J Neurosci 23: 2502-2510.

8. Békésy Gv (1939) Über die Vibrationsempfindung. Akustische Zeitschrift 4: 316-334.

9. Benison AM, Ard TD, Crosby AM, Barth DS (2006) Temporal Patterns of Field Potentials in Vibrissa/Barrel Cortex Reveal Stimulus Orientation and Shape. J Neurophysiol 95: 2242-2251.

10. Bermejo R, Harvey M, Gao P, Zeigler HP (1996) Conditioned whisking in the rat. Somatosens Mot Res 13: 225-233.

11. Bermejo R, Szwed M, Friedman W, Ahissar E, Zeigler HP (2004) One whisker whisking: unit recording during conditioned whisking in rats. Somatosens Mot Res 21: 183-187.

12. Blackwell HR (1952) Studies of psychophysical methods for measuring visual thresholds. J Opt Soc Am 42: 606-616.

13. Blough D, Blough P (1977) Animal psychophysics. In: Handbook of operant behavior (Honig WK, Staddon JER, eds), Englewood Cliffs, New Jersey: Prentice-Hall.

14. Bolanowski SJ, Jr., Gescheider GA, Verrillo RT, Checkosky CM (1988) Four channels mediate the mechanical aspects of touch. J Acoust Soc Am 84: 1680-1694.

15. Brecht M, Preilowski B, Merzenich MM (1997) Functional architecture of the mystacial vibrissae. Behav Brain Res 84: 81-97.

16. Britten KH, Newsome WT, Shadlen MN, Celebrini S, Movshon JA (1996) A relationship between behavioral choice and the visual responses of neurons in macaque MT. Vis Neurosci 13: 87-100.

17. Britten KH, Shadlen MN, Newsome WT, Movshon JA (1992) The analysis of visual motion: a comparison of neuronal and psychophysical performance. J Neurosci 12: 4745-4765.

18. Capraro AJ, Verrillo RT, Zwislocki JJ (1979) Psychophysical evidence for a triplex system of cutaneous mechanoreception. Sens Processes 3: 334-352.

19. Carvell GE, Simons DJ (1988) Membrane potential changes in rat SmI cortical neurons evoked by controlled stimulation of mystacial vibrissae. Brain Res 448: 186-191.

20. Carvell GE, Simons DJ (1990) Biometric analyses of vibrissal tactile discrimination in the rat. J Neurosci 10: 2638-2648.

21. Carvell GE, Simons DJ (1995) Task- and subject-related differences in sensorimotor behavior during active touch. Somatosens Mot Res 12: 1-9.

22. Chen LM, Friedman RM, Ramsden BM, LaMotte RH, Roe AW (2001) Fine-scale organization of SI (area 3b) in the squirrel monkey revealed with intrinsic optical imaging. J Neurophysiol 86: 3011-3029.

23. Chung S, Li X, Nelson SB (2002) Short-term depression at thalamocortical synapses contributes to rapid adaptation of cortical sensory responses in vivo. Neuron 34: 437-446.

24. Cohen J (1994) The earth is round ($p<.05$). American Psychologist 49: 997-1003.

25. Cumming G, Finch S (2001) A primer on the understanding, use, and calculation of confidence intervals that are based on central and noncentral distributions. Educational and Psychological Measurement 61: 532-574.

26. Cureton EE (1956) Rank-biserial correlation. Psychometrika 21: 287-290.

27. de Lafuente V, Romo R (2005) Neuronal correlates of subjective sensory experience. Nat Neurosci 8: 1698-1703.

28. De Valois RL, Abramov I, Mead WR (1967) Single cell analysis of wavelength discrimination at the lateral geniculate nucleus in the macaque. J Neurophysiol 30: 415-433.

29. Deschenes M, Timofeeva E, Lavallee P (2003) The relay of high-frequency sensory signals in the Whisker-to-barreloid pathway. J Neurosci 23: 6778-6787.

30. Ebara S, Kumamoto K, Matsuura T, Mazurkiewicz JE, Rice FL (2002) Similarities and differences in the innervation of mystacial vibrissal follicle-sinus complexes in the rat and cat: a confocal microscopic study. J Comp Neurol 449: 103-119.

31. Fanselow EE, Nicolelis MA (1999) Behavioral modulation of tactile responses in the rat somatosensory system. J Neurosci 19: 7603-7616.

32. Faul F, Erdfelder E, Lang A-G, Buchner A (in press) G*Power 3: A flexible statistical power analysis program for the social, behavioral, and biomedical sciences. Behavior Research Methods.

33. Friedman RM, Chen LM, Roe AW (2004) Modality maps within primate somatosensory cortex. Proc Natl Acad Sci U S A 101: 12724-12729.

34. Gao P, Ploog BO, Zeigler HP (2003) Whisking as a "voluntary" response: operant control of whisking parameters and effects of whisker denervation. Somatosens Mot Res 20: 179-189.

35. Geisler WS, Albrecht DG (1997) Visual cortex neurons in monkeys and cats: detection, discrimination, and identification. Vis Neurosci 14: 897-919.

36. Gescheider GA, Bolanowski SJ, Pope JV, Verrillo RT (2002) A four-channel analysis of the tactile sensitivity of the fingertip: frequency selectivity, spatial summation, and temporal summation. Somatosens Mot Res 19: 114-124.

37. Gescheider GA, Bolanowski SJ, Verrillo RT (2004) Some characteristics of tactile channels. Behav Brain Res 148: 35-40.

38. Gescheider GA, Sklar BF, Van Doren CL, Verrillo RT (1985) Vibrotactile forward masking: psychophysical evidence for a triplex theory of cutaneous mechanoreception. J Acoust Soc Am 78: 534-543.

39. Gibson JM, Welker WI (1983) Quantitative studies of stimulus coding in first-order vibrissa afferents of rats. 1. Receptive field properties and threshold distributions. Somatosens Res 1: 51-67.

40. Goldstein EB (1997) Wahrnehmungspsychologie. Heidelberg: Spektrum Akademischer Verlag.

41. Griffiths WJ (1960) Responses of wild and domestic rats to forced swimming. Psychological Reports 6: 39-49.

42. Guic-Robles E, Jenkins WM, Bravo H (1992) Vibrissal roughness discrimination is barrelcortex-dependent. Behav Brain Res 48: 145-152.

43. Guic-Robles E, Valdivieso C, Guajardo G (1989) Rats can learn a roughness discrimination using only their vibrissal system. Behav Brain Res 31: 285-289.

44. Gustafson JW, Felbain-Keramidas SL (1977) Behavioral and neural approaches to the function of the mystacial vibrissae. Psychological Bulletin 84: 477-488.

45. Hall CS (1934) Emotional behavior in the rat. I. Defecation and urination as measures of individual differences in emotionality. Journal of Comparative Psychology 18: 385-403.

46. Harvey MA, Bermejo R, Zeigler HP (2001) Discriminative whisking in the head-fixed rat: optoelectronic monitoring during tactile detection and discrimination tasks. Somatosens Mot Res 18: 211-222.

47. Hentschke H, Haiss F, Schwarz C (2006) Central signals rapidly switch tactile processing in rat barrel cortex during whisker movements. Cereb Cortex 16: 1142-1156.

48. Hermle T, Schwarz C, Bogdan M (2004) Employing ICA and SOM for spike sorting of multielectrode recordings from CNS. J Physiol Paris 98: 349-356.

49. Hernandez A, Zainos A, Romo R (2000) Neuronal correlates of sensory discrimination in the somatosensory cortex. Proc Natl Acad Sci U S A 97: 6191-6196.

50. Hipp J, Arabzadeh E, Zorzin E, Conradt J, Kayser C, Diamond ME, Konig P (2006) Texture signals in whisker vibrations. J Neurophysiol 95: 1792-1799.

51. Hutson KA, Masterton RB (1986) The sensory contribution of a single vibrissa's cortical barrel. J Neurophysiol 56: 1196-1223.

52. Ito M, Kato M (2002) Analysis of variance study of the rat cortical layer 4 barrel and layer 5b neurones. J Physiol 539: 511-522.

53. Jacquin MF, Renehan WE, Rhoades RW, Panneton WM (1993) Morphology and topography of identified primary afferents in trigeminal subnuclei principalis and oralis. J Neurophysiol 70: 1911-1936.

54. Jakel F, Wichmann FA (2006) Spatial four-alternative forced-choice method is the preferred psychophysical method for naive observers. J Vis 6: 1307-1322.

55. Johansson RS, Birznieks I (2004) First spikes in ensembles of human tactile afferents code complex spatial fingertip events. Nat Neurosci 7: 170-177.

56. Johansson RS, Vallbo AB (1979) Detection of tactile stimuli. Thresholds of afferent units related to psychophysical thresholds in the human hand. J Physiol 297: 405-422.

57. Johnson KO, Darian-Smith I, LaMotte C (1973) Peripheral neural determinants of temperature discrimination in man: a correlative study of responses to cooling skin. J Neurophysiol 36: 347-370.

58. Johnson KO, Lamb GD (1981) Neural mechanisms of spatial tactile discrimination: neural patterns evoked by braille-like dot patterns in the monkey. J Physiol 310: 117-144.

59. Johnson KO, Yoshioka T, Vega-Bermudez F (2000) Tactile functions of mechanoreceptive afferents innervating the hand. J Clin Neurophysiol 17: 539-558.

60. Jones EG, Diamond IT (1995) The barrel cortex of rodents. New York: Plenum Press.

61. Jones LM, Kwegyir-Afful EE, Keller A (2006) Whisker primary afferents encode temporal frequency of moving gratings. Somatosens Mot Res 23: 45-54.

62. Jones LM, Depireux DA, Simons DJ, Keller A (2004a) Robust temporal coding in the trigeminal system. Science 304: 1986-1989.

63. Jones LM, Lee S, Trageser JC, Simons DJ, Keller A (2004b) Precise Temporal Responses in Whisker Trigeminal Neurons. J Neurophysiol.

64. Kandel ER, Schwartz JH, Jessell TM (2000) Principles of neural science. New York: McGraw-Hill.

65. Kerr JN, Greenberg D, Helmchen F (2005). Imaging input and output of neocortical networks in vivo. Proc Natl Acad Sci U S A 102:14063-14068.

66. Kline RB (2004) Beyond significance testing. Washington,DC: American Psychological Association.

67. Knutsen PM, Pietr M, Ahissar E (2006) Haptic object localization in the vibrissal system: behavior and performance. J Neurosci 26: 8451-8464.

68. Krupa DJ, Matell MS, Brisben AJ, Oliveira LM, Nicolelis MA (2001) Behavioral properties of the trigeminal somatosensory system in rats performing whisker-dependent tactile discriminations. J Neurosci 21: 5752-5763.

69. LaMotte RH, Mountcastle VB (1975) Capacities of humans and monkeys to discriminate vibratory stimuli of different frequency and amplitude: a correlation between neural events and psychological measurements. J Neurophysiol 38: 539-559.

70. Leiser SC, Moxon KA (2007) Responses of Trigeminal Ganglion Neurons during Natural Whisking Behaviors in the Awake Rat. Neuron 53: 117-133.

71. Lichtenstein SH, Carvell GE, Simons DJ (1990) Responses of rat trigeminal ganglion neurons to movements of vibrissae in different directions. Somatosens Mot Res 7: 47-65.

72. Luna R, Hernandez A, Brody CD, Romo R (2005) Neural codes for perceptual discrimination in primary somatosensory cortex. Nat Neurosci 8: 1210-1219.

73. Mehta SB, Whitmer D, Figueroa R, Williams BA, Kleinfeld D (2007) Active spatial perception in the vibrissa scanning sensorimotor system. PLoS Biol 5: e15.

74. Milani H, Steiner H, Huston JP (1989) Analysis of recovery from behavioral asymmetries induced by unilateral removal of vibrissae in the rat. Behav Neurosci 103: 1067-1074.

75. Möck M, Butovas S, Schwarz C (2006) Functional unity of the ponto-cerebellum: evidence that intrapontine communication is mediated by a reciprocal loop with the cerebellar nuclei. J Neurophysiol 95: 3414-3425.

76. Moore CI, Nelson SB (1998) Spatio-temporal subthreshold receptive fields in the vibrissa representation of rat primary somatosensory cortex. J Neurophysiol 80: 2882-2892.

77. Mountcastle VB, LaMotte RH, Carli G (1972) Detection thresholds for stimuli in humans and monkeys: comparison with threshold events in mechanoreceptive afferent nerve fibers innervating the monkey hand. J Neurophysiol 35: 122-136.

78. Mountcastle VB, Steinmetz MA, Romo R (1990) Frequency discrimination in the sense of flutter: psychophysical measurements correlated with postcentral events in behaving monkeys. J Neurosci 10: 3032-3044.

79. Mountcastle VB, Talbot WH, Darian-Smith I, Kornhuber HH (1967) Neural basis of the sense of flutter-vibration. Science 155: 597-600.

80. Mountcastle VB, Talbot WH, Sakata H, Hyvarinen J (1969) Cortical neuronal mechanisms in flutter-vibration studied in unanesthetized monkeys. Neuronal periodicity and frequency discrimination. J Neurophysiol 32: 452-484.

81. Ochoa J, Torebjork E (1983) Sensations evoked by intraneural microstimulation of single mechanoreceptor units innervating the human hand. J Physiol 342: 633-654.

82. Parker AJ, Newsome WT (1998) Sense and the single neuron: probing the physiology of perception. Annu Rev Neurosci 21: 227-277.

83. Paul RL, Merzenich M, Goodman H (1972) Representation of slowly and rapidly adapting cutaneous mechanoreceptors of the hand in Brodmann's areas 3 and 1 of Macaca mulatta. Brain Res 36: 229-249.

84. Penfield W, Rasmussen T (1950) The cerebral cortex of man. New York: Macmillan.

85. Petersen CC (2003) The barrel cortex–integrating molecular, cellular and systems physiology. Pflugers Arch 447: 126-134.

86. Pinto DJ, Brumberg JC, Simons DJ (2000) Circuit dynamics and coding strategies in rodent somatosensory cortex. J Neurophysiol 83: 1158-1166.

87. Powell TP, Mountcastle VB (1959) Some aspects of the functional organization of the cortex of the postcentral gyrus of the monkey: a correlation of findings obtained in a single unit analysis with cytoarchitecture. Bull Johns Hopkins Hosp 105: 133-162.

88. Prigg T, Goldreich D, Carvell GE, Simons DJ (2002) Texture discrimination and unit recordings in the rat whisker/barrel system. Physiol Behav 77: 671-675.

89. Richter CP (1957) On the phenomenon of sudden death in animals and man. Psychosom Med 19: 191-198.

90. Rieke F, Warland D, de Ruyter van Steveninck RR, Bialek W (1997) Spikes: Exploring the neural code. Cambridge: MIT Press.

91. Romo R, Salinas E (2003) Flutter discrimination: neural codes, perception, memory and decision making. Nat Rev Neurosci 4: 203-218.

92. Sachdev RNS, Jenkinson E, Zeigler HP, Ebner FF (2001) Sensorimotor plasticity in the rodent vibrissa system. In: The Mutable Brain (Kaas JH, ed), pp 123-164. Amsterdam: Harwood Academic Publishers.

93. Sakitt B (1972) Counting every quantum. J Physiol 223: 131-150.

94. Schiffman HR, Lore R, Passafiume J, Neeb R (1970) Role of vibrissae for depth perception in the rat (rattus norvegicus). Animal Behaviour 18: 290-292.

95. Shadlen MN, Britten KH, Newsome WT, Movshon JA (1996) A computational analysis of the relationship between neuronal and behavioral responses to visual motion. J Neurosci 16: 1486-1510.

96. Shipley MT (1974) Response characteristics of single units in the rat's trigeminal nuclei to vibrissa displacements. J Neurophysiol 37: 73-90.

97. Shoykhet M, Doherty D, Simons DJ (2000) Coding of deflection velocity and amplitude by whisker primary afferent neurons: implications for higher level processing. Somatosens Mot Res 17: 171-180.

98. Simons DJ (1983) Multi-whisker stimulation and its effects on vibrissa units in rat SmI barrel cortex. Brain Res 276: 178-182.

99. Simons DJ (1985) Temporal and spatial integration in the rat SI vibrissa cortex. J Neurophysiol 54: 615-635.

100. Simons DJ, Carvell GE (1989) Thalamocortical response transformation in the rat vibrissa/barrel system. J Neurophysiol 61: 311-330.

101. Simons DJ, Carvell GE, Hershey AE, Bryant DP (1992) Responses of barrel cortex neurons in awake rats and effects of urethane anesthesia. Exp Brain Res 91: 259-272.

102. Sretavan D, Dykes RW (1983) The organization of two cutaneous submodalities in the forearm region of area 3b of cat somatosensory cortex. J Comp Neurol 213: 381-398.

103. Stanislaw H, Todorov N (1999) Calculation of signal detection theory measures. Behav Res Methods Instrum Comput 31: 137-149.

104. Stüttgen MC, Rüter J, Schwarz C (2006) Two psychophysical channels of whisker deflection in rats align with two neuronal classes of primary afferents. J Neurosci 26: 7933-7941.

105. Sur M, Wall JT, Kaas JH (1981) Modular segregation of functional cell classes within the postcentral somatosensory cortex of monkeys. Science 212: 1059-1061.

106. Sur M, Wall JT, Kaas JH (1984) Modular distribution of neurons with slowly adapting and rapidly adapting responses in area 3b of somatosensory cortex in monkeys. J Neurophysiol 51: 724-744.

107. Swadlow HA (1995) Influence of VPM afferents on putative inhibitory interneurons in S1 of the awake rabbit: evidence from cross-correlation, microstimulation, and latencies to peripheral sensory stimulation. J Neurophysiol 73: 1584-1599.

108. Swets JA (1961) Detection theory and psychophysics: a review. Psychometrika 26: 49-63.

109. Szwed M, Bagdasarian K, Ahissar E (2003) Encoding of vibrissal active touch. Neuron 40: 621-630.

110. Szwed M, Bagdasarian K, Blumenfeld B, Barak O, Derdikman D, Ahissar E (2006) Responses of trigeminal ganglion neurons to the radial distance of contact during active vibrissal touch. J Neurophysiol 95: 791-802.

111. Talbot WH, Darian-Smith I, Kornhuber HH, Mountcastle VB (1968) The sense of flutter-vibration: comparison of the human capacity with response patterns of mechanoreceptive afferents from the monkey hand. J Neurophysiol 31: 301-334.

112. Tanner WP, Jr., Swets JA (1954) A decision-making theory of visual detection. Psychol Rev 61: 401-409.

113. Tolhurst DJ, Movshon JA, Dean AF (1983) The statistical reliability of signals in single neurons in cat and monkey visual cortex. Vision Res 23: 775-785.

114. Treitel L (1897) Über das Vibrationsgefühl der Haut. Archiv für Psychiatrie und Nervenkrankheiten 29: 633-640.

115. Vallbo AB, Olsson KA, Westberg KG, Clark FJ (1984) Microstimulation of single tactile afferents from the human hand. Sensory attributes related to unit type and properties of receptive fields. Brain 107 (Pt 3): 727-749.

116. Verrillo RT (1963) Effect of contactor area on the vibrotactile threshold. J Acoust Soc Am 35: 1962-1966.

117. Verrillo RT (1965) Temporal summation in vibrotactile sensitivity. J Acoust Soc Am 37: 843-846.

118. Verrillo RT (1966) Vibrotactile sensitivity and the frequency response of Pacinian corpuscles. Psychonomic Science 4: 135-136.

119. Vincent SB (1912) The function of the vibrissae in the behavior of the white rat. Behavior Monographs 1: 1-86.

120. Vogels R, Orban GA (1990) How well do response changes of striate neurons signal differences in orientation: a study in the discriminating monkey. J Neurosci 10: 3543-3558.

121. Webber RM, Stanley GB (2004) Nonlinear encoding of tactile patterns in the barrel cortex. J Neurophysiol 91: 2010-2022.

122. Welker C (1971) Microelectrode delineation of fine grain somatotopic organization of (SmI) cerebral neocortex in albino rat. Brain Res 26: 259-275.

123. Welker WI (1964) Analysis of sniffing of the albino rat. Behaviour 22: 223-244.

124. Welsh JP (1998) Systemic harmaline blocks associative and motor learning by the actions of the inferior olive. Eur J Neurosci 10: 3307-3320.

125. Woolsey TA, van der Loos H (1970) The structural organization of layer IV in the somatosensory region (SI) of mouse cerebral cortex. The description of a cortical field composed of discrete cytoarchitectonic units. Brain Res 17: 205-242.

126. Zhu JJ, Connors BW (1999) Intrinsic firing patterns and whisker-evoked synaptic responses of neurons in the rat barrel cortex. J Neurophysiol 81: 1171-1183.

127. Zucker E, Welker WI (1969) Coding of somatic sensory input by vibrissae neurons in the rat's trigeminal ganglion. Brain Res 12: 138-156.

Appendix: Animal care statement

The studies included in present dissertation were performed to investigate the neurophysiology of the rat whisker system. The experiments described here required the use of laboratory rats (*Rattus norvegicus)*. All procedures in the described experiments were conducted as to impose minimum suffering and provide maximum comfort to preserve animals' health and well being by the allowed methods available to date. All experimental protocols were approved by the responsible regulatory institution (Regierungspräsidium Tübingen) and carried out in accordance with the policy on the use of animals in neuroscience research of the Society for Neuroscience and German national law.

Erklärungen

Ich erkläre hiermit,

1. dass ich bisher keine Promotions- oder entsprechende Prüfungsverfahren abgebrochen oder abgeschlossen habe.

2. dass die vorgelegte Dissertation noch nie ganz oder teilweise als Dissertation oder sonstige Prüfungsarbeit eingereicht worden ist und …..

   - auch nicht ganz oder teilweise veröffentlicht worden ist.

   - ***oder**:* bereits teilweise in den angegebenen Zeitschriften veröffentlicht wurde:
     Alle Abbildungen in Kapitel 2 sowie ein Großteil des Textes beruht auf:
     Stüttgen, Rüter, Schwarz (2007). The Journal of Neuroscience 26(30): 7933-7941.
     Copyright 2006 by the Society for Neuroscience.

3. dass ich die zur Promotion eingereichte Arbeit mit dem Titel: „Psychophysical Channels and the Physiology of Perception in the Rat Whisker System" selbstständig verfasst, nur die angegebenen Quellen und Hilfsmittel benutzt und wörtlich oder inhaltlich übernommene Stellen als solche gekennzeichnet habe. Ich versichere an Eides statt, dass diese Angaben wahr sind und dass ich nichts verschwiegen habe. Mir ist bekannt, dass die falsche Abgabe einer Versicherung an Eides statt mit Freiheitsstrafe bis zu drei Jahren oder mit Geldstrafe bestraft wird.

4. dass ich bisher weder strafrechtlich verurteilt, noch Disziplinarmaßnahmen und anhängigen Straf- und Disziplinarverfahren unterzogen worden bin.

Tübingen, den 17.10.2007 …….

(Unterschrift)